the local TiO_6 octahedron predicted from both the π-bonding arguments and the comparative overlap populations conflicts with observation, these computational results affirm the importance of O–O interactions in controlling the bond distances in TiO_2. Other local geometrical features, for example, the planarity of each OTi_3 unit, are also controlled by the π-interactions between Ti and O.

Our conclusions from this study are severalfold. There is not dramatic structural change concerning the metal coordination polyhedra as the temperature is lowered. The overall result is a small shrinkage in the metric of the lattice for both anatase and rutile. No large changes in bond lengths and angles are observed in contrast to those we have described for the open framework of cristobalite.[14] There is a small effect in anatase associated with the oxygen atom movement. Indeed in these close-packed structures these are the sorts of changes that should be expected. Only in more open structures should changes in the hinging of coordination polyhedra be found as the temperature is changed. However, the sense of the coordination geometry about the metal is the same at both temperatures and shows that the structure is clearly controlled by a balance of attractive Ti–O and repulsive O–O forces.

Acknowledgment. This research was supported by a generous grant to J.K.B. from the Dow Chemical Co. and by the National Science Foundation through Grant NSF DMR8276892 to the Materials Research Laboratory at The University of Chicago. J.W.R. acknowledges support of the Intense Pulsed Neutron Source By DoE, Contract W-31-109-ENG-38. This study is relevant to the attempt to understand the bonding of open-framework structures supporrted by Grant NSF CHE 84-05167. We also acknowledge J. D. Jorgensen of Argonne National Laboratory and J. J. Pluth and I. D. Steele for their experimental assistance.

Appendix

The tight-binding calculations were performed within the framework of the extended Hückel approach.[26] All Ti–O distances were set at 1.95 Å in both polymorphs. The geometry at oxygen was fixed by angles of 90°, 90°, and 135° in rutile and 155.8°, 102.1°, and 102.1° in anatase for the plots of Figure 4. The density of states curves were calculated by averaging over 40 special points in the irreducible wedge of the first Brillouin zone for the simple tetragonal lattice. Parameters for Ti and O were those used in the earlier study.[11] The plots of Figure 4a,b were obtained by variation of the u parameter of anatase while the Ti–O distance was kept fixed in an analogous way to the approach used in ref 11. The molecular mechanics calculations on anatase and rutile employed a finite cluster model consisting of nine unit cells of the crystal arranged in a tetragonal prism. The interaction energy of the four and eight oxide ions, respectively, in rutile and anatase, located in the central cell with the ions of all nine cells, was evaluated by using a simple Lennard-Jones potential with a minimum at 2.99 Å. With this requirement the shape of the curve is completely determined, but the energy units are arbitrary. We do not feel that trying to weight the energetic importance of the "electronic" and "hard sphere" effects is a useful exercise using our methods. The interaction energy was of sufficiently short range that this size prism was very adequate for this purpose. A two-dimensional energy surface in the coordinates u (which fixes the oxygen atoms positions in both structures) and the distortion coordinate q around the metal ion was constructed. If r_a, r_t, and r_f are respectively the average metal–oxygen distance and the distances of the symmetry-equivalent pair and quartet of distances in the real structure, then the distortion coordinate was that which kept the average metal–oxygen distance constant, i.e., $r_t = r_a + q$ and $r_f = r_a - (q/2)$.

Registry No. TiO_2, 13463-67-7.

Calcium-Selective Ligands. 2.[1] Structural and Spectroscopic Studies on Calcium and Cadmium Complexes of $EGTA^{4-}$

Cynthia K. Schauer and Oren P. Anderson*

Contribution from the Department of Chemistry, Colorado State University, Fort Collins, Colorado 80523. *Received August 1, 1986*

Abstract: The structures of salts of the calcium and cadmium complexes of the octadentate ligand $EGTA^{4-}$, Ca[Ca(EGTA)]·($^{22}/_3$)H_2O (**1**) and Sr[Cd(EGTA)]·7H_2O (**2**), have been investigated by single-crystal X-ray diffraction. **1** crystallizes in the monoclinic space group $P2_1/c$ (Z = 12), with a = 24.358 (4) Å, b = 16.798 (4) Å, c = 19.015 (4) Å, and β = 94.05 (2)°. **2** crystallizes in the monoclinic space group $P2_1/n$ (Z = 4), with a = 16.814 (4) Å, b = 8.454 (2) Å, c = 17.614 (5) Å, and β = 97.34 (2)°. Both Ca^{2+} and Cd^{2+} utilize the octadentate chelating capability of $EGTA^{4-}$ to form anions exhibiting distorted dodecahedral coordination spheres. In $[Ca(EGTA)]^{2-}$ anions, the nitrogen atoms bind to Ca^{2+} at longer distances (Ca–N(av) = 2.60 (2) Å) than do the ether oxygen atoms (Ca–O(ether, av) = 2.50 (3) Å) or the carboxylate oxygen atoms (Ca–O(carb, av) = 2.38 (2) Å). In $[Cd(EGTA)]^{2-}$, however, the nitrogen atoms bind to Cd^{2+} at shorter distances (Cd–N (av) = 2.43 (1) Å) than do the ether oxygen atoms (Cd–O(ether, av) = 2.580 (8) Å). The carboxylate oxygen atoms still bind at the shortest distances (Cd–O(carb, av) = 2.35 (5) Å). ^1H NMR spectra of the $[Ca(EGTA)]^{2-}$ and $[Cd(EGTA)]^{2-}$ anions show that in each case all carboxylate groups are made equivalent by intramolecular exchange at room temperature. The effect of dissociation of nitrogen ligand atoms, with subsequent inversion at nitrogen, is evident in ^1H NMR spectra for $[Ca(EGTA)]^{2-}$ at elevated temperatures. The ^{113}Cd chemical shift for $[Cd(EGTA)]^{2-}$ in solution (+15 ppm) reflects a more shielded environment for the ^{113}Cd nucleus than does the chemical shift (+36 ppm) for solid **2**. The ^{113}Cd powder pattern of **2** yields the three components of the shielding tensor (σ_{11} = +159, σ_{22} = +29, σ_{33} = −81 ppm); the most highly shielded component occurs in the range typical of cadmium-substituted calcium-binding proteins.

Structural aspects of the chelation of metal ions by highly polydentate ligands (i.e., ligands containing six or more binding sites) have recently become of interest in this laboratory. Many ligands in this category exhibit interesting patterns of metal-binding selectivity, yet, with the exception of $EDTA^{4-}$ (H_4EDTA = 3,6-bis(carboxymethyl)-3,6-diazaoctanedioic acid), little systematic structural knowledge exists regarding the manner in which such ligands bind to metals.

One important example of such selectivity is associated with the alkaline earth metal ions, Mg^{2+}–Ba^{2+}. In the body, mobile calcium (i.e., nonmineral calcium) is bound at a variety of sites

(1) Part 1: Schauer, C. K.; Anderson, O. P. *Acta Crystallogr., Sec. C: Cryst. Struct. Commun.* **1986**, *C42*, 760.

0002-7863/87/1509-3646$01.50/0

and participates in a number of important processes (muscle contraction, blood clotting, neurotransmitter release, hormonal response, etc.). A typical cell maintains a high gradient of Ca^{2+} concentration across the membrane (≈0.1 μM inside, vs. ≈2 mM outside) as well as a high internal preponderance of Mg^{2+} (≈0.1 mM).

Such factors allow the use of calcium ion as a second messenger within the cell. In this process, a stimulus at the cell's outer surface is thought to cause binding sites on the interior of the cell membrane to release Ca^{2+}, increasing the concentration of Ca^{2+} in the cytosol by a factor of 10–20. Intracellular proteins containing binding sites with an affinity for Ca^{2+} of appropriate magnitude ($K_d \approx 10^{-7}$ M) and a high degree of selectivity for binding Ca^{2+} over Mg^{2+} (>10^4 difference in stability constants) bind the Ca^{2+} thus released. The resulting change in protein conformation allows the metalloprotein to participate in processes such as those mentioned above.

Troponin C and calmodulin are examples of such calcium-binding proteins, with central roles in the regulation of important biological processes.[2-12] Troponin C plays a fundamental role in muscle contraction,[13] while calmodulin regulates ATPase activity,[14] exocytosis,[15,16] and other cellular functions.[4-7] Structural studies on troponin C[17,18] and calmodulin[19] have not yet reached the resolution needed to be confident of details such as the coordination number and geometric arrangement about the calcium ions in the helix-loop-helix calcium-binding domains. A related protein, carp muscle parvalbumin, contains two calcium-binding domains,[20] commonly referred to as EF hands.[10] In one of these two sites, a calcium ion is bound by six ligand atoms, including oxygen atoms from unidentate carboxylate groups of aspartic (Asp) and glutamic (Glu) acid residues, a serine hydroxyl group, and an amido oxygen atom of a phenylalanine residue. In the second site, a calcium ion is bound by eight ligand atoms, including both unidentate and bidentate carboxylate groups from Asp and Glu residues, an amido oxygen atom of a lysine residue, and the oxygen atom of a single water molecule. The proposal that similar domains perform the highly selective calcium complexation characteristic of other calcium-binding proteins[10] has received apparent confirmation from the X-ray diffraction studies of troponin C[17,18] and calmodulin.[19]

Table I. Stability Constants

ligand	log K Mg^{2+}	Ca^{2+}	Sr^{2+}	Ba^{2+}	Cd^{2+}	ref
calmodulin	3.0	6.0–7.2				29, 30
$EDTA^{4-}$	8.8	10.7	8.7	7.9	16.4	31
$EGTA^{4-}$	5.2	11.0	8.5	8.4	16.7	31
$BAPTA^{4-}$	1.8	7.0				32

Information regarding the structures of the calcium-binding sites in the native calcium-binding proteins is difficult to obtain by using techniques other than X-ray crystallography, due to the calcium ion's lack of useful spectroscopic properties. Although ^{43}Ca NMR signals have been observed for calcium-binding proteins,[21,22] expensive isotopic enrichment is required, and the signals obtained are broad. Consequently, other metals have been substituted for Ca^{2+} as spectroscopic probes of binding site structure. The Cd^{2+} ion[23,24] (as a ^{113}Cd NMR probe) and various tripositive lanthanide ions (as ^1H NMR shift reagents as well as EPR and luminescence probes)[25-28] have been used in this manner. Such metal ions, of course, may bind to the calcium-binding site in a significantly different manner than does Ca^{2+}. To date, structural studies have not explored the differences in coordination that occur when such metals are substituted for calcium in a highly selective calcium-binding site.

The structural features of the calcium-binding site that are associated with the high calcium-binding selectivity of the proteins remain unknown. Several factors may contribute to the ability of the proteins to bind Ca^{2+} selectively, among which are the following: (1) differences in size and preferred coordination number among the alkaline earth metals, (2) different ligand atom preferences among the metals, and (3) steric constraints of the binding site. The degree to which such factors contribute to calcium-binding selectivity may be explored in complexes of calcium-selective ligands such as $EGTA^{4-}$ (H_4EGTA = 3,12-bis(carboxymethyl)-6,9-dioxa-3,12-diazatetradecanedioic acid).

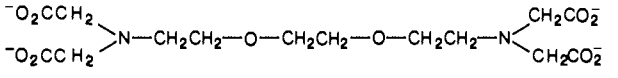

$EGTA^{4-}$

The $EGTA^{4-}$ ligand is highly selective toward Ca^{2+} among the alkaline earth metal ions. In fact, its preference for the binding of Ca^{2+} over Mg^{2+} (~10^6) is even larger than that typically exhibited by calcium-binding proteins (see Table I). Calcium-binding proteins also complex Sr^{2+} and Ba^{2+} ions more weakly than Ca^{2+};[33] the $EGTA^{4-}$ ligand's selectivity at this end of the alkaline earth series is reflected in the fact that the stability constant for $[Ca(EGTA)]^{2-}$ is ~10^3 larger than the stability constants for the strontium and barium complexes. As a result of this high degree of selectivity, $EGTA^{4-}$ can deplete the concentration of Ca^{2+} without influencing the concentration of Mg^{2+}; this property has been useful in biological studies of calcium function.[34] Earlier studies[35] employed $EDTA^{4-}$ for the same purpose, despite its much lower degree of selectivity for calcium

(2) *Calcium in Biology*; Spiro, T. G., Ed.; J. Wiley and Sons: New York, 1983.
(3) *Calcium and Its Role in Biology*; Sigel, H., Ed.; Marcel Dekker: New York, 1984.
(4) Cheung, W. Y. *Science (Washington, DC)* **1980**, *207*, 19.
(5) *Calcium and Cell Function*; Cheung, W. Y., Ed.; Academic Press: New York, 1980; Vol. 1.
(6) *Calcium and Cell Function*; Cheung, W. Y., Ed.; Academic Press: New York, 1982; Vol. 2.
(7) Campbell, A. K. *Intracellular Calcium*; John Wiley & Sons: New York, 1983.
(8) *Calcium Binding Proteins, 1983*; DeBernard, B., Sottocasa, G. L., Sandri, G., Carafoli, E., Taylor, A. N., Vanaman, T. C., Williams, R. J. P., Eds.; Elsevier: New York, 1983.
(9) *Calcium Binding Proteins: Structure and Function*; Siegel, F. L., Carafoli, E., Kretsinger, R. H., Mackennan, D. H., Wasserman, R. H., Eds.; Elsevier: North Holland, New York, 1980.
(10) Kretsinger, R. H. *CRC Crit. Rev. Biochem.* **1980**, 119.
(11) *Calmodulin and Cell Function*; Watterson, D. M., Vincenzi, F. F., Eds.; New York Academy of Science: 1980.
(12) Means, A. R.; Tash, J. R.; Chafouleas, J. G. *Physiol. Rev.* **1982**, *62*, 1.
(13) Ashley, C. C. in ref 2, Chapter 3, p 107.
(14) Cormier, M. J. in ref 2, Chapter 2, p 55.
(15) Rubin, R. P. in ref 2, Chapter 4, p 175.
(16) Creutz, C. E. in ref 3, Chapter 8, p 319.
(17) Sundaralingam, M.; Bergstrom, R.; Strasburg, G.; Rao, S. T.; Roychowdhury, P.; Greaser, M.; Wang, B. C. *Science (Washington, DC)* **1985**, *227*, 945.
(18) Herzberg, O.; James, M. N. G. *Nature (London)* **1985**, *313*, 653.
(19) Babu, Y. S.; Sack, J. S.; Greenhough, T. J.; Bugg, C. E.; Means, A. R.; Cook, W. J. *Nature (London)* **1985**, *315*, 37.
(20) Moews, P. C.; Kretsinger, R. H. *J. Mol. Biol.* **1975**, *91*, 201.
(21) Vogel, H. J.; Drakenberg, T.; Forsēn, S. In *NMR of Newly Accessible Nuclei*; Lazlo, P., Ed.; Academic Press: New York, 1983; Vol. I, Chapter 7, p 157.
(22) Andersson, T.; Drakenberg, T.; Forsēn, S.; Thulin, E.; Sward, M. *J. Am. Chem. Soc.* **1982**, *104*, 576.
(23) Armitage, I. M.; Boulanger, Y. *NMR of Newly Accessible Nuclei*; Lazlo, P., Ed.; Academic Press: New York, 1983; Vol. II, Chapter 13, p 337.
(24) Ellis, P. D. *Science (Washington, DC)* **1983**, *221*, 1141.
(25) Martin, R. B. in ref 2, Chapter 6, p 235.
(26) Nieboer, E. *Struct. Bonding (Berlin)* **1975**, *22*, 1.
(27) Horrocks, W.; Albin, M. *Prog. Inorg. Chem.* **1984**, *31*, 1.
(28) Richardson, F. S. *Chem. Rev.* **1982**, *82*, 541.
(29) Klee, C. B.; Vanaman, T. C. *Adv. Protein Chem.* **1982**, *35*, 213.
(30) Haiech, J.; Klee, C. B.; Demaille, J. G. *Biochemistry* **1981**, *20*, 3890.
(31) Martell, A. E.; Smith, R. M. *Critical Stability Constants*; Plenum Press: New York, 1974; Vol. I.
(32) Tsien, R. Y. *Biochemistry* **1980**, *19*, 2396.
(33) Seamon, K. B.; Kretsinger, R. H. in ref 2, Chapter 1, p 20.
(34) Reference 7, Chapter 2.
(35) Portzehl, H.; Caldwell, P. C.; Ruegg, J. C. *Biochim. Biophys. Acta* **1964**, *79*, 581.

(see Table I). Recently, $BAPTA^{4-}$, an EGTA-like ligand (in which 1,2-disubstituted benzene rings link the amino nitrogen atoms to the ether oxygen atoms) with a similar degree of calcium-binding selectivity has been used as a calcium ion buffer, due to its lower dependence of stability on pH and more rapid complexation of Ca^{2+}.[32]

The high calcium-binding selectivity exhibited by $EGTA^{4-}$ makes the $[M(EGTA)]^{2-}$ system (M^{2+} = Mg^{2+}–Ba^{2+}) of interest as a model for the binding sites in the calcium-binding proteins. In fact, similarities exist between the coordination environments common in calcium-binding proteins and that provided by the $EGTA^{4-}$ ligand. In parvalbumin, troponin C, and calmodulin, the high affinity binding sites contain only oxygen donors and bear an overall charge of −4, due to the presence of four carboxylate groups. Six of the eight ligand atoms of $EGTA^{4-}$ are neutral or anionic oxygen donors, and the overall charge of the $EGTA^{4-}$ ligand is identical with the charges on the protein binding sites.

The structural features that are associated with the ability of $EGTA^{4-}$ to bind calcium in a highly selective fashion are not known. In this work, the results of single-crystal X-ray diffraction studies on $Ca[Ca(EGTA)]\cdot(^{22}/_3)H_2O$ (hereafter **1**) and $Sr[Cd(EGTA)]\cdot 7H_2O$ (hereafter **2**) are reported. The structure of the calcium complex has been determined in order to establish the coordination geometry about Ca^{2+} in the highly calcium-selective environment provided by the $EGTA^{4-}$ ligand. The structure of the cadmium complex has been determined in order to establish the nature and magnitude of the structural changes that take place when Cd^{2+} is substituted for Ca^{2+} in such an environment. In addition, the relationship between the structures of $[Ca(EGTA)]^{2-}$ and $[Cd(EGTA)]^{2-}$ in solution and the structures of these complex anions in the solid state has been explored by variable temperature ^1H NMR studies and by ^{113}Cd NMR studies (solution and solid state). It is hoped that a more complete picture of the structural basis for the calcium selectivity exhibited by ligands such as $EGTA^{4-}$ will assist in understanding similar properties of calcium-binding proteins.

Experimental Section

All reagents were used as purchased ($Ca(OH)_2$ (Fisher), $CdCO_3$ (Fisher), H_4EGTA (J. T. Baker), $Sr(OH)_2\cdot 8H_2O$ (Alfa)).

Synthesis of $Ca[Ca(EGTA)]\cdot(^{22}/_3)H_2O$, 1. $Ca(OH)_2$ (0.148 g, 2.00 mmol) was added to an aqueous slurry (20 mL) of H_4EGTA (0.385 g, 1.01 mmol). The solids dissolved on warming and stirring. The pH of the resultant solution was adjusted to 9, by using a small amount of $Ca(OH)_2$. Addition of 30 mL of acetone, followed by slow cooling of the solution to refrigerator temperature, resulted in the growth of single crystals suitable for the X-ray diffraction study. The clear, colorless plates were characterized by the structure determination as well as by NMR spectroscopy: ^1H NMR (D_2O, 200 MHz, pH 9, DDS standard, δ, ppm) (2.82, t, 4, $^3J_{HH}$ = 4.7 Hz), (3.25, AB_q, 8, J_{AB} = 14 Hz), (3.62, t, 4, $^3J_{HH}$ = 4.7 Hz), (3.77, s, 4); ^{13}C NMR (D_2O, 68 MHz, pH 9, DDS standard, δ, ppm) (58.89, t, $^1J_{CH}$ = 137 Hz), (63.25, t, $^1J_{CH}$ = 136 Hz), (69.52, t, $^1J_{CH}$ = 144 Hz), (70.51, t, $^1J_{CH}$ = 146 Hz), (181.91, s).

Synthesis of $Sr[Cd(EGTA)]\cdot 7H_2O$, 2. $Sr(OH)_2\cdot 8H_2O$ (0.265 g, 1.00 mmol) and $CdCO_3$ (0.172 g, 1.00 mmol) were added to a stirred aqueous slurry (6 mL) of H_4EGTA (0.380 g, 1.00 mmol), yielding a neutral solution upon warming. Addition of 14 mL of acetone, followed by slow cooling of the solution to room temperature, resulted in isolation of single crystals (clear, colorless, nearly equidimensional parallelepipeds) suitable for the X-ray diffraction study. The compound was characterized by the structure determination as well as by ^1H NMR spectroscopy. The ^1H NMR spectrum of $[Cd(EGTA)]^{2-}$ has been previously reported;[36] the ^1H NMR spectrum of **2** agreed with the spectrum in that report.

NMR Experiments. ^1H NMR spectra were obtained at various temperatures from solutions of $Na_2[Ca(EGTA)]$ (pH 9, 0.1 M) and $Na_2[Cd(EGTA)]$ (pH 9, 0.1 M) on a Bruker WP-200 spectrometer equipped with a variable temperature probe. The pH values of the solutions were chosen to ensure that the concentration of HML^- was negligible in each case.

The natural abundance ^{113}Cd NMR spectrum from a solution of $Na_2[Cd(EGTA)]$ (pH 9, 0.1 M) was recorded at 44.4 MHz on the same spectrometer, utilizing a 10-mm tube, a tunable broad-band probe, and 0.10 M $Cd(ClO_4)_2$ as reference. ^{113}Cd NMR spectra (spinning and nonspinning) from an unenriched sample of solid **2** were obtained on a Nicolet NT-200 spectrometer at 44.4 MHz, with $Cd(ClO_4)_2\cdot 6H_2O$ as reference. Standard cross-polarization conditions (2 ms contact time) were utilized (^1H decoupling field 42 kHz, 1-s delay between scans). A rotor speed of 1.8 kHz was utilized in acquisition of the magic-angle spinning spectrum.

Table II. Crystallographic Experiments and Computations

compd	1	2
formula	$C_{14}H_{20}Ca_2N_2O_{10}\cdot(^{22}/_3)H_2O$	$C_{14}H_{20}CdN_2O_{10}Sr\cdot 7H_2O$
formula wt, amu	588.54	702.44
temp, °C	20 (1)	20 (1)
cryst system	monoclinic	monoclinic
space group	$P2_1/c$	$P2_1/n$
a, Å	24.358 (4)	16.814 (4)
b, Å	16.798 (4)	8.454 (2)
c, Å	19.015 (4)	17.614 (5)
β, deg	94.05 (2)	97.34 (2)
V, Å^3	7761	2483
Z	12	4
$F(000)$	3736	1416
D_{calcd}, g cm^{-3}	1.51	1.88
cryst dim, mm	0.15 × 0.4 × 0.4	0.38 (001 → 00$\bar{1}$) × 0.40 (100 → $\bar{1}$00) × 0.44 (010 → 0$\bar{1}$0)
radiatn	Mo Kα (λ = 0.7107 Å)	Mo Kα
monochromator	graphite	graphite
μ, cm^{-1}	4.90	31.70
scan type	$\theta/2\theta$	$\theta/2\theta$
2θ range, deg	3.5–50.0	3.5–50.0
indices collctd	$+h,+k,\pm l$	$\pm h,+k,-l$
reflecns	14674 measd	4882 measd
	13702 unique	4394 unique
	9136 used ($I > 2.5\sigma(I)$)	3713 used ($I > 2.5\sigma(I)$)
scan spd, deg min^{-1}	1.98–29.30	1.98–29.30
no. least sq params	973	316
data/params	9.4	11.8
R^a	0.068	0.032
$R_w{}^a$	0.073	0.036
GOF^a	1.89	1.21
g	1.2 × 10^{-3}	1.0 × 10^{-3}
slope, norm prob plot^b	1.47	1.00

$^a R = (\sum||F_o| - |F_c||)/(\sum|F_o|)$; $R_w = \{(\sum w(|F_o| - |F_c|)^2)/(\sum w(F_o)^2)\}^{1/2}$; GOF = $\{(\sum w(|F_o| - |F_c|)^2)/(N_{data} - N_{params})\}^{1/2}$. ^{b}Abrahams, S. C. *Acta Crystallograllogr., Sect. B: Struct. Crystallogr. Cryst. Chem.* **1974**, *B30*, 261–268.

Structure Determination for $Ca[Ca(EGTA)]\cdot(^{22}/_3)H_2O$, 1. Crystal data for **1**, together with details of the X-ray diffraction experiment and subsequent computations, are given in Table II. The unit cell dimensions were obtained from a least-squares fit to the setting angles for 25 reflections (2θ(ave) = 20.2°) on a Nicolet R3m diffractometer.[37] Calculation of a reasonable density required 12 formula units per unit cell. Due to the rarity of such a result in $P2_1/c$, an attempt was made to find an alternative cell by using TRACER;[38] none was discovered. The stability of the crystal was monitored by measurement of the intensities of three reflections (200, 0$\bar{8}$0, 00$\bar{5}$) every 100 data points. The intensities of these three reflections declined by an average of 11% during data collection; a correction for this decay was applied (in addition to Lorentz and polarization corrections) during data reduction. No correction was made for absorption, due to the small average value of μt.

The initial E-map (using phases supplied by the direct methods routine SOLV[37]) revealed the positions of six Ca^{2+} ions. Neutral atom scattering factors[39] and anomalous scattering contributions[40] were used for all atoms. Subsequent Fourier difference electron density maps revealed all non-hydrogen ligand atoms, oxygen atoms of water molecules coordinated

(36) Reed, G. H.; Kula, R. J. *Inorg. Chem.* **1971**, *10*, 2050.

(37) Software used for diffractometer operations and data collection was provided with the Nicolet R3m diffractometer. Crystallographic computations were carried out with the SHELXTL program library, written by G. M. Sheldrick and supplied by Nicolet XRD for the Data General Eclipse S/140 computer in the crystallography laboratory at Colorado State University.

(38) The general cell reduction program TRACER, originally written by S. L. Lawton, was obtained from J. A. Ibers, Northwestern University.

(39) *International Tables for X-ray Crystallography*; Kynoch Press: Birmingham, England, 1974; Vol. IV, p 99.

(40) *International Tables for X-ray Crystallography*; Kynoch Press: Birmingham, England, 1974; Vol. IV, p 149.

Table III. Atomic Coordinates ($\times 10^4$) and Isotropic Thermal Parameters ($Å^2 \times 10^3$)[a] for $Ca[Ca(EGTA)]\cdot(^{22}/_3)H_2O$

atom	x	y	z	U_{iso}[b]	atom	x	y	z	U_{iso}[b]
Ca1	1538 (1)	11479 (1)	4187 (1)	26 (1)	N6	4309 (2)	12556 (3)	3108 (3)	36 (2)
Ca2	1611 (1)	8445 (1)	1149 (1)	24 (1)	O1	2401 (2)	10858 (3)	4062 (2)	46 (2)
Ca3	4707 (1)	11366 (1)	2465 (1)	35 (1)	O2	3105 (2)	10570 (3)	3434 (3)	53 (2)
Ca4	−24 (1)	12459 (1)	162 (1)	26 (1)	O3	987 (2)	12314 (2)	3405 (2)	35 (1)
Ca5	465 (1)	9934 (1)	2529 (1)	30 (1)	O4	825 (2)	13014 (3)	2422 (2)	47 (2)
Ca6	3788 (1)	9675 (1)	3169 (1)	33 (1)	O5	1913 (2)	12828 (2)	4505 (2)	38 (1)
C1	2399 (3)	11382 (4)	2906 (3)	40 (2)	O6	1952 (2)	11565 (2)	5410 (2)	39 (1)
C2	2656 (2)	10908 (4)	3514 (3)	37 (2)	O7	1136 (2)	10379 (2)	3524 (2)	34 (1)
C3	1681 (3)	12360 (4)	2587 (3)	37 (2)	O8	989 (2)	9090 (2)	3414 (2)	41 (1)
C4	1126 (2)	12592 (3)	2822 (3)	31 (2)	O9	733 (2)	11617 (2)	4803 (2)	32 (1)
C5	2419 (3)	12678 (4)	3460 (4)	43 (2)	O10	175 (2)	11177 (2)	5580 (2)	35 (1)
C6	2122 (3)	13242 (4)	3909 (4)	42 (2)	O11	2474 (2)	9029 (3)	1435 (2)	38 (1)
C7	2302 (3)	12822 (4)	5114 (3)	46 (2)	O12	3087 (2)	9503 (3)	2244 (2)	41 (1)
C8	2053 (3)	12353 (4)	5675 (3)	45 (2)	O13	1062 (2)	7584 (2)	1797 (2)	34 (1)
C9	1764 (3)	11038 (4)	5927 (3)	43 (2)	O14	909 (2)	6809 (3)	2710 (2)	46 (2)
C10	1737 (3)	10224 (4)	5578 (3)	41 (2)	O15	2006 (2)	7076 (2)	901 (2)	38 (1)
C11	1458 (3)	9538 (3)	4488 (3)	35 (2)	O16	2066 (2)	8341 (2)	28 (2)	37 (1)
C12	1172 (2)	9677 (3)	3758 (3)	29 (2)	O17	1211 (2)	9533 (2)	1742 (2)	35 (1)
C13	782 (3)	10243 (3)	5115 (3)	33 (2)	O18	1001 (2)	10810 (2)	1789 (2)	42 (1)
C14	555 (2)	11076 (3)	5186 (3)	26 (2)	O19	814 (2)	8394 (2)	355 (2)	32 (1)
C15	2452 (3)	8530 (4)	2606 (3)	37 (2)	O20	257 (2)	8903 (3)	−486 (2)	39 (1)
C16	2697 (2)	9047 (4)	2055 (3)	33 (2)	O21	5156 (2)	12312 (3)	1772 (2)	52 (2)
C17	1744 (2)	7524 (4)	2757 (3)	34 (2)	O22	5406 (3)	12718 (3)	729 (3)	97 (3)
C18	1207 (3)	7278 (3)	2390 (3)	31 (2)	O23	4321 (2)	10067 (3)	2208 (2)	41 (1)
C19	2504 (3)	7243 (4)	2040 (3)	39 (2)	O24	4154 (2)	9061 (3)	1466 (3)	49 (2)
C20	2219 (3)	6673 (4)	1527 (3)	41 (2)	O25	5576 (2)	10663 (4)	2638 (3)	79 (2)
C21	2373 (3)	7065 (4)	354 (4)	45 (2)	O26	5369 (2)	11948 (3)	3375 (3)	54 (2)
C22	2137 (3)	7561 (4)	−243 (3)	42 (2)	O27	3859 (2)	11824 (3)	1930 (3)	52 (2)
C23	1919 (3)	8921 (4)	−494 (3)	41 (2)	O28	3338 (3)	12868 (3)	1623 (3)	77 (2)
C24	1918 (3)	9725 (4)	−133 (3)	37 (2)	O29	4291 (2)	10914 (2)	3498 (2)	42 (1)
C25	1575 (3)	10391 (3)	890 (3)	31 (2)	O30	3999 (2)	11298 (3)	4529 (3)	64 (2)
C26	1245 (2)	10240 (3)	1514 (3)	29 (2)	w1	−686 (2)	12664 (3)	1016 (2)	42 (1)
C27	941 (3)	9763 (3)	51 (3)	35 (2)	w2	−451 (2)	13271 (3)	−788 (2)	42 (1)
C28	657 (2)	8963 (3)	−35 (3)	28 (2)	w3	428 (2)	11698 (3)	−717 (2)	45 (2)
C29	5006 (4)	11445 (5)	786 (4)	80 (4)	w4	640 (2)	12206 (3)	1119 (2)	42 (1)
C30	5209 (4)	12218 (4)	1124 (4)	63 (3)	w5	120 (2)	11258 (3)	2879 (3)	55 (2)
C31	4578 (3)	10190 (4)	1029 (4)	50 (2)	w6	−304 (2)	9655 (3)	3207 (3)	62 (2)
C32	4335 (3)	9737 (4)	1606 (4)	38 (2)	w7	176 (2)	8582 (3)	2156 (3)	52 (2)
C33	5523 (4)	10417 (7)	1420 (6)	94 (5)	w8	−242 (2)	10112 (3)	1604 (3)	65 (2)
C34	5632 (5)	10081 (8)	2023 (9)	61 (5)	w9	3327 (3)	8963 (4)	4087 (3)	81 (2)
C34′	5937 (8)	10665 (13)	1998 (11)	70 (8)	w10	4582 (3)	9250 (4)	3900 (4)	112 (3)
C35	6012 (4)	11035 (7)	3039 (6)	114 (5)	w11	3946 (2)	8321 (3)	2721 (3)	60 (2)
C36	5796 (4)	11434 (5)	3648 (5)	78 (4)	w12	3083 (2)	759 (3)	1237 (3)	64 (2)
C37	5156 (3)	12464 (4)	3888 (4)	55 (3)	w13	3051 (2)	4446 (4)	1592 (3)	77 (2)
C38	4748 (3)	13002 (4)	3495 (4)	46 (2)	w14	3132 (2)	172 (4)	5098 (3)	81 (3)
C39	4023 (3)	13036 (4)	2564 (4)	47 (2)	w15	3321 (3)	8724 (5)	476 (4)	112 (3)
C40	3708 (3)	12537 (4)	1997 (4)	51 (2)	w16	3721 (3)	2378 (5)	272 (3)	106 (3)
C41	3919 (3)	12210 (4)	3582 (4)	42 (2)	w17	3420 (3)	4157 (5)	4863 (4)	109 (3)
C42	4092 (3)	11426 (4)	3901 (3)	39 (2)	w18	2380 (3)	4933 (5)	2663 (4)	121 (4)
N1	2064 (2)	12043 (3)	3142 (3)	31 (2)	w19	3097 (3)	5218 (6)	3863 (5)	138 (4)
N2	1363 (2)	10220 (3)	4937 (2)	28 (1)	w20	1270 (3)	5072 (6)	2736 (6)	154 (5)
N3	2135 (2)	7859 (3)	2279 (2)	31 (2)	w21	3562 (5)	7427 (10)	4619 (8)	301 (9)
N4	1495 (2)	9732 (3)	392 (2)	31 (2)	w22	4445 (8)	4806 (10)	351 (10)	301 (12)
N5	4984 (2)	10788 (3)	1287 (3)	44 (2)	w23	6660 (11)	11944 (18)	1490 (17)	78 (12)

[a] Esd's in the least significant digits are given in parentheses. [b] For these values, the equivalent isotropic U is defined as $^1/_3$ of the trace of the U_{ij} tensor.

to calcium counterions, and oxygen atoms of occluded water molecules.

Resolvable disorder was seen at one position (C34, C34′) of the backbone of one of the three $EGTA^{4-}$ ligands. Refinement of the site occupancy factor for C34 yielded a final value of 0.62 (1). High values were exhibited for thermal parameters of oxygen atoms of three occluded water molecules (w21, w22, w23); refinement of site occupancy factors for these atoms yielded values significantly less than 1.0 only for w22 (0.81 (3)) and w23 (0.21 (2)). The values of the site occupancy factors for these two atoms were fixed at 0.8 and 0.2 during the final refinement cycles. Interpretation of residual electron density as oxygen atoms of occluded water molecules was terminated at a level of 1 e $Å^{-3}$.

Although hydrogen atoms of water molecules were visible in the ΔF map, they were not included in the final structural model. All non-hydrogen atoms were given anisotropic thermal parameters. Hydrogen atoms of the $EGTA^{4-}$ ligands were included in idealized positions (C–H = 0.96 Å, $U(H) = 1.2U_{iso}(C)$). The weighted refinement ($w = [\sigma^2(F_o) + |g|F_o^2]^{-1}$) on F converged ($(\text{shift/esd})_{av} < 0.068$ over the last 10 cycles) to yield the R values in Table II. In the final ΔF map, the highest peaks (1 e $Å^{-3}$) occurred near occluded water molecules; the minimum in the map was −0.5 e $Å^{-3}$.

Final fractional atomic coordinates for all non-hydrogen atoms of **1** are listed in Table III. Metric parameters relevant to the chelated calcium ions, the partially aquated Ca^{2+} counterions, and the interionic interactions between these species are listed in Table IV (parts a, b, and c, respectively). Ligand structural parameters (Table V) have also been tabulated.

Structure Determination for $Sr[Cd(EGTA)]\cdot 7H_2O$, 2. Crystal data for **2**, together with details of the X-ray diffraction experiment and subsequent calculations, are given in Table II. The unit cell dimensions were obtained from a least-squares fit to the setting angles of 24 reflections ($2\theta(\text{ave}) = 18.8°$). The intensities of three reflections (1200, 040, 0012) were measured every 100 reflections. No significant change in the intensities of these reflections was noted during data collection. An empirical absorption correction was performed, utilizing the intensity profiles obtained for 14 reflections as a function of Ψ ($\Delta\Psi = 15°$). The range of transmission factors exhibited for the complete data set was ±6% of the mean value. Lorentz and polarization corrections were applied to the data.

Analysis of the Patterson map established the positions of the Sr^{2+} and Cd^{2+} ions. Subsequent ΔF electron density maps revealed all non-hy-

Table IV. Metal–Ligand Distances (Å) and Angles (deg)[a] for $Ca[Ca(EGTA)]\cdot(^{22}/_{3})H_2O$

a. Complex Ions

complex a				complex b				complex c			
Ca1–N1	2.617 (5)	Ca1–O5	2.502 (4)	Ca2–N3	2.613 (5)	Ca2–O15	2.550 (4)	Ca3–N5	2.575 (6)	Ca3–O25	2.426 (6)
Ca1–N2	2.603 (5)	Ca1–O6	2.473 (4)	Ca2–N4	2.602 (5)	Ca2–O16	2.477 (4)	Ca3–N6	2.567 (5)	Ca3–O26	2.483 (5)
Ca1–O1	2.375 (5)	Ca1–O7	2.404 (4)	Ca2–O11	2.347 (4)	Ca2–O17	2.392 (4)	Ca3–O21	2.379 (5)	Ca3–O27	2.365 (5)
Ca1–O3	2.386 (4)	Ca1–O9	2.365 (4)	Ca2–O13	2.374 (4)	Ca2–O19	2.375 (4)	Ca3–O23	2.412 (4)	Ca3–O29	2.397 (5)
N1–Ca1–N2	144.9 (2)	O5–Ca1–O6	66.5 (1)	N3–Ca2–N4	142.7 (1)	O15–Ca2–O16	65.2 (1)	N5–Ca3–N6	147.0 (2)	O25–Ca3–O26	65.1 (2)
N1–Ca1–O1	66.3 (2)	N1–Ca1–O7	94.8 (1)	N3–Ca2–O11	65.8 (1)	N3–Ca2–O17	95.2 (1)	N5–Ca3–O21	67.1 (2)	N5–Ca3–O27	91.3 (2)
N2–Ca1–O1	83.0 (2)	N2–Ca1–O7	65.6 (1)	N4–Ca2–O11	80.8 (1)	N4–Ca2–O17	66.0 (1)	N6–Ca3–O21	87.0 (2)	N6–Ca3–O27	66.7 (2)
N1–Ca1–O3	66.3 (1)	O1–Ca1–O7	86.6 (1)	N3–Ca2–O13	66.7 (1)	O11–Ca2–O17	87.6 (1)	N5–Ca3–O23	66.7 (2)	O21–Ca3–O27	88.1 (2)
N2–Ca1–O3	135.5 (1)	O3–Ca1–O7	86.3 (1)	N4–Ca2–O13	138.6 (1)	O13–Ca2–O17	87.5 (1)	N6–Ca3–O23	130.2 (2)	O23–Ca3–O27	83.7 (2)
O1–Ca1–O3	131.2 (2)	O5–Ca1–O7	161.9 (1)	O11–Ca2–O13	131.5 (1)	O15–Ca2–O17	161.5 (1)	O21–Ca3–O23	132.8 (2)	O25–Ca3–O27	160.7 (2)
N1–Ca1–O5	70.4 (1)	O6–Ca1–O7	131.4 (1)	N3–Ca2–O15	69.1 (1)	O16–Ca2–O17	133.0 (1)	N5–Ca3–O25	69.8 (2)	O26–Ca3–O27	132.6 (2)
N2–Ca1–O5	132.4 (1)	N1–Ca1–O9	143.9 (1)	N4–Ca2–O15	132.4 (1)	N3–Ca2–O19	147.0 (1)	N6–Ca3–O25	132.0 (2)	N5–Ca3–O29	138.2 (2)
O1–Ca1–O5	96.4 (1)	N2–Ca1–O9	68.6 (1)	O11–Ca2–O15	94.4 (1)	N4–Ca2–O19	68.1 (1)	O21–Ca3–O25	88.3 (2)	N6–Ca3–O29	70.2 (2)
O3–Ca1–O5	78.3 (1)	O1–Ca1–O9	149.7 (2)	O13–Ca2–O15	77.4 (1)	O11–Ca2–O19	147.2 (1)	O23–Ca3–O25	84.9 (2)	O21–Ca3–O29	154.5 (2)
N1–Ca1–O6	120.2 (1)	O3–Ca1–O9	78.6 (1)	N3–Ca2–O16	117.4 (1)	O13–Ca2–O19	80.9 (1)	N5–Ca3–O26	123.9 (2)	O23–Ca3–O29	72.4 (1)
N2–Ca1–O6	66.6 (1)	O5–Ca1–O9	95.3 (1)	N4–Ca2–O16	67.7 (1)	O15–Ca2–O19	98.7 (1)	N6–Ca3–O26	67.0 (2)	O25–Ca3–O29	98.6 (2)
O1–Ca1–O6	79.3 (1)	O6–Ca1–O9	79.9 (1)	O11–Ca2–O16	77.4 (1)	O16–Ca2–O19	81.1 (1)	O21–Ca3–O26	79.7 (2)	O26–Ca3–O29	81.0 (2)
O3–Ca1–O6	136.5 (1)	O7–Ca1–O9	90.8 (1)	O13–Ca2–O16	135.0 (1)	O17–Ca2–O19	89.2 (1)	O23–Ca3–O26	136.3 (2)	O27–Ca3–O29	92.8 (2)

b. Counterions

counterion 1				counterion 2				counterion 3			
Ca4–w1	2.393 (5)	Ca4–O9a	2.540 (4)	Ca5–O7	2.526 (4)	Ca5–w5	2.485 (5)	Ca6–O2	2.325 (5)	Ca6–w9	2.452 (6)
Ca4–w2	2.437 (4)	Ca4–O10a	2.461 (4)	Ca5–O8	2.485 (4)	Ca5–w6	2.395 (5)	Ca6–O12	2.381 (4)	Ca6–w10	2.408 (7)
Ca4–w3	2.430 (5)	Ca4–O19a	2.542 (4)	Ca5–O17	2.525 (4)	Ca5–w7	2.467 (5)	Ca6–O23	2.407 (5)	Ca6–w11	2.469 (5)
Ca4–w4	2.386 (4)	Ca4–O20a	2.447 (4)	Ca5–O18	2.470 (5)	Ca5–w8	2.392 (5)	Ca6–O29	2.473 (4)		
w1–Ca4–w2	98.6 (2)	O9a–Ca4–O10a	52.3 (1)	O7–Ca5–O8	52.1 (1)	w5–Ca5–w6	74.9 (2)	O2–Ca6–O12	75.6 (2)	w9–Ca6–w10	80.5 (2)
w1–Ca4–w3	154.5 (2)	w1–Ca4–O19a	79.3 (1)	O7–Ca5–O17	93.9 (1)	O7–Ca5–w7	130.1 (1)	O2–Ca6–O23	114.9 (2)	O2–Ca6–w11	143.3 (2)
w2–Ca4–w3	88.5 (1)	w2–Ca4–O19a	75.9 (1)	O8–Ca5–O17	83.8 (1)	O8–Ca5–w7	78.0 (1)	O12–Ca6–O23	82.5 (1)	O12–Ca6–w11	75.8 (2)
w1–Ca4–w4	87.8 (2)	w3–Ca4–O19a	78.7 (1)	O7–Ca5–O18	84.9 (1)	O17–Ca5–w7	77.7 (1)	O2–Ca6–O29	75.6 (2)	O23–Ca6–w11	83.4 (2)
w2–Ca4–w4	153.6 (2)	w4–Ca4–O19a	130.5 (1)	O8–Ca5–O18	117.3 (2)	O18–Ca5–w7	122.4 (2)	O12–Ca6–O29	127.3 (1)	O29–Ca6–w11	140.9 (2)
w3–Ca4–w4	96.7 (2)	O9a–Ca4–O19a	141.7 (1)	O17–Ca5–O18	52.5 (1)	w5–Ca5–w7	143.7 (2)	O23–Ca6–O29	71.2 (1)	w9–Ca6–w11	83.5 (2)
w1–Ca4–O9a	129.2 (1)	O10a–Ca4–O19a	140.9 (1)	O7–Ca5–w5	75.4 (1)	w6–Ca5–w7	75.9 (2)	O2–Ca6–w9	77.9 (2)	w10–Ca6–w11	77.7 (2)
w2–Ca4–O9a	74.8 (1)	w1–Ca4–O20a	77.5 (1)	O8–Ca5–w5	119.8 (2)	O7–Ca5–w8	155.3 (2)	O12–Ca6–w9	97.2 (2)		
w3–Ca4–O9a	76.3 (1)	w2–Ca4–O20a	127.9 (1)	O17–Ca5–w5	132.0 (2)	O8–Ca5–w8	151.4 (2)	O23–Ca6–w9	166.5 (2)		
w4–Ca4–O9a	81.3 (1)	w3–Ca4–O20a	78.8 (1)	O18–Ca5–w5	79.7 (2)	O17–Ca5–w8	96.3 (2)	O29–Ca6–w9	118.3 (2)		
w1–Ca4–O10a	76.9 (1)	w4–Ca4–O20a	78.4 (1)	O7–Ca5–w6	98.3 (2)	O18–Ca5–w8	83.6 (2)	O2–Ca6–w10	128.7 (2)		
w2–Ca4–O10a	77.5 (1)	O9a–Ca4–O20a	145.6 (1)	O8–Ca5–w6	84.7 (2)	w5–Ca5–w8	81.1 (2)	O12–Ca6–w10	153.5 (2)		
w3–Ca4–O10a	128.6 (1)	O10a–Ca4–O20a	146.4 (1)	O17–Ca5–w6	152.8 (2)	w6–Ca5–w8	82.5 (2)	O23–Ca6–w10	93.8 (2)		
w4–Ca4–O10a	79.2 (1)	O19a–Ca4–O20a	52.2 (1)	O18–Ca5–w6	152.6 (2)	w7–Ca5–w8	74.2 (2)	O29–Ca6–w10	74.9 (2)		

c. Interionic Angles

Ca6–O2–C2	164.9 (4)	C14–O10–Ca4b	94.1 (3)	C28–O19–Ca4a	90.5 (3)	Ca5–O8–C12	92.9 (3)	Ca5–O17–C26	91.1 (3)	Ca6–O23–C32	127.8 (4)
Ca1–O7–Ca5	146.9 (2)	Ca6–O12–C16	140.9 (4)	C28–O20–Ca4a	94.9 (3)	Ca1–O9–Ca4b	146.7 (2)	Ca5–O18–C26	93.9 (3)	Ca3–O29–Ca6	106.8 (2)
Ca5–O7–C12	90.7 (3)	Ca2–O17–Ca5	144.8 (2)	Ca3–O23–Ca6	108.5 (2)	C14–O9–Ca4b	89.9 (3)	Ca2–O19–Ca4a	146.1 (2)	Ca6–O29–C42	121.2 (4)

[a] Esd's in the least significant digits are given in parentheses.

Table V. Chelate Ring[a] Bonding Parameters[b] for $Ca[Ca(EGTA)]\cdot(^{22}/_{3})H_2O$

Glycinate Rings

	C–C′	C′–N	C–O	C–O′	C–C′–N
G1	1.504 (9)	1.466 (8)	1.254 (8)	1.249 (8)	112.1 (5)
G2	1.503 (9)	1.460 (7)	1.272 (7)	1.240 (7)	115.0 (5)
G3	1.527 (8)	1.456 (7)	1.261 (7)	1.247 (7)	109.5 (5)
G4	1.514 (8)	1.479 (8)	1.261 (7)	1.243 (7)	114.0 (5)
G5	1.515 (9)	1.478 (8)	1.265 (7)	1.252 (7)	111.4 (5)
G6	1.497 (8)	1.475 (8)	1.267 (7)	1.257 (7)	113.6 (5)
G7	1.500 (8)	1.460 (7)	1.269 (7)	1.260 (7)	109.3 (5)
G8	1.515 (8)	1.457 (8)	1.254 (7)	1.255 (7)	114.8 (5)
G9	1.516 (11)	1.461 (10)	1.257 (9)	1.247 (10)	113.3 (6)
G10	1.492 (10)	1.470 (9)	1.273 (8)	1.240 (7)	113.3 (6)
G11	1.528 (10)	1.451 (8)	1.262 (9)	1.239 (9)	113.0 (5)
G12	1.498 (9)	1.474 (9)	1.270 (8)	1.250 (8)	114.8 (5)

	O–C–O′	C′–C–O	C′–C–O′	Ca–N–C′	Ca–O–C
G1	124.0 (6)	118.1 (5)	117.9 (6)	105.7 (3)	123.2 (4)
G2	124.2 (6)	117.6 (5)	118.1 (5)	111.0 (3)	125.9 (4)
G3	122.8 (5)	118.6 (5)	118.6 (5)	106.1 (3)	121.3 (3)
G4	123.4 (5)	118.1 (5)	118.2 (5)	107.5 (3)	123.2 (3)
G5	123.4 (6)	117.9 (5)	118.6 (5)	105.6 (3)	123.0 (4)
G6	123.5 (5)	118.8 (5)	117.6 (5)	110.6 (3)	125.3 (4)
G7	121.6 (5)	118.7 (5)	119.7 (5)	105.4 (3)	121.0 (4)
G8	122.3 (5)	119.6 (5)	118.1 (5)	109.6 (3)	123.4 (3)
G9	125.2 (7)	118.1 (7)	116.7 (7)	107.8 (4)	122.7 (5)
G10	124.1 (6)	118.4 (5)	117.5 (6)	109.7 (4)	122.8 (4)
G11	125.0 (7)	117.1 (6)	117.8 (6)	105.8 (4)	121.2 (4)
G12	124.3 (6)	117.3 (5)	118.2 (6)	105.4 (3)	118.8 (4)

Amino Ether Rings

	C–C′	C–N	C′–O	C–C′–O	C′–C–N
A1	1.496 (9)	1.474 (8)	1.452 (8)	110.6 (5)	113.5 (5)
A2	1.519 (9)	1.467 (7)	1.422 (8)	105.3 (5)	111.9 (5)
A3	1.501 (9)	1.464 (8)	1.435 (7)	111.2 (5)	112.8 (5)
A4	1.514 (8)	1.484 (8)	1.418 (7)	107.8 (5)	109.6 (5)
A5	1.29 (2)	1.46 (1)	1.54 (2)	112.3 (12)	118.0 (10)
A6	1.50 (1)	1.461 (8)	1.430 (9)	106.6 (5)	112.1 (5)

	C″–N–C†	C–N–C″	C–N–C†	Ca–N–C	Ca–O–C′
A1	113.3 (5)	110.5 (5)	111.1 (5)	104.8 (4)	112.8 (3)
A2	110.3 (4)	112.1 (4)	110.9 (5)	109.6 (3)	119.0 (3)
A3	111.9 (4)	110.9 (5)	111.0 (5)	106.6 (3)	113.0 (3)
A4	109.8 (4)	112.1 (5)	111.5 (4)	108.2 (3)	116.6 (4)
A5	110.7 (6)	111.1 (7)	110.1 (6)	107.4 (5)	109.3 (6)
A6	110.9 (5)	111.8 (5)	112.0 (5)	110.7 (4)	117.7 (4)

Diether Rings

	C–C′	C′–O′	C–O	C′–C–O	C–C′–O′
E1	1.49 (1)	1.431 (8)	1.444 (8)	107.5 (5)	107.8 (5)
E2	1.491 (9)	1.422 (7)	1.418 (8)	108.8 (5)	106.8 (5)
E3	1.47 (2)	1.42 (1)	1.41 (1)	109.2 (8)	106.5 (8)

	C′–O′–C†	C″–O–C	Ca–O–C	Ca–O′–C′
E1	112.8 (5)	112.4 (5)	113.3 (3)	115.8 (3)
E2	114.3 (4)	113.2 (5)	114.4 (3)	116.7 (3)
E3	114.3 (6)	125.8 (8)	118.4 (6)	115.9 (5)

[a] Chelate ring designations have been assigned systematically, as follows. Within each series, rings are numbered according to increasing oxygen atom number. For glycinate rings, C′ is adjacent to N, and O′ is the carboxylate oxygen atom not bound to the metal in the EGTA chelate. Within amino ether rings, C′ is adjacent to O, and C is adjacent to N; C″ and C† are also attached to N, with C″ possessing the lower number of these two atoms. Within diether rings, C′ is bound to O′ (always odd numbered), and C is bound to O; C″ is also bound to O, and C† is bound to O′. [b] Bond lengths are given in Å, and bond angles are given in deg. Esd's in the least significant digits are given in parentheses.

drogen ligand atoms and the oxygen atoms of seven water molecules (four of which were bound to the partially aquated Sr^{2+} cation). In the final structural model, all non-hydrogen atoms were given anisotropic thermal parameters. Hydrogen atoms of the $EGTA^{4-}$ ligand were included as in the structural model for **1**. At convergence (weighted least squares refinement on F, $(\text{shift/esd})_{av} < 0.052$ over the last four cycles) the final ΔF map exhibited a maximum of 0.67 e Å^{-3} in the immediate vicinity of Cd^{2+} and a minimum of −0.35 e Å^{-3}.

Table VI. Atomic Coordinates ($\times 10^4$) and Isotropic Thermal Parameters (Å$^2 \times 10^3$)[a] for $Sr[Cd(EGTA)]\cdot 7H_2O$

atom	x	y	z	U_{iso}[b]
Cd	7566 (1)	617 (1)	106 (1)	31 (1)
Sr	9211 (1)	5310 (1)	804 (1)	36 (1)
C1	6360 (3)	−1953 (5)	535 (2)	39 (1)
C2	6166 (2)	−1746 (4)	−333 (2)	35 (1)
C3	7078 (3)	−801 (5)	1697 (2)	43 (1)
C4	7804 (3)	205 (5)	1910 (2)	35 (1)
C5	5974 (3)	613 (5)	948 (3)	44 (1)
C6	6252 (3)	2288 (5)	1117 (3)	44 (1)
C7	6188 (3)	3648 (5)	−80 (3)	46 (1)
C8	6700 (3)	4046 (5)	−688 (3)	43 (1)
C9	7528 (3)	2786 (5)	−1504 (2)	42 (1)
C10	7816 (3)	1161 (5)	−1694 (2)	39 (1)
C11	8291 (3)	−1369 (5)	−1190 (2)	38 (1)
C12	8428 (2)	−2396 (5)	−473 (2)	37 (1)
C13	9051 (2)	990 (5)	−808 (2)	37 (1)
C14	9089 (2)	2373 (4)	−259 (2)	31 (1)
N1	6658 (2)	−490 (4)	926 (2)	35 (1)
N2	8248 (2)	325 (4)	−1026 (2)	33 (1)
O1	6523 (2)	−653 (4)	−648 (2)	46 (1)
O2	5687 (2)	−2695 (4)	−670 (2)	48 (1)
O3	8155 (2)	765 (4)	1386 (2)	47 (1)
O4	8048 (2)	367 (4)	2607 (2)	47 (1)
O5	6690 (2)	2869 (3)	528 (2)	40 (1)
O6	6992 (2)	2591 (3)	−944 (2)	39 (1)
O7	8348 (2)	−1794 (4)	161 (2)	43 (1)
O8	8597 (2)	−3826 (3)	−571 (2)	45 (1)
O9	8514 (2)	2622 (3)	117 (2)	36 (1)
O10	9713 (2)	3207 (3)	−182 (2)	40 (1)
w1	9365 (3)	2885 (6)	1675 (2)	102 (2)
w2	10657 (2)	5257 (4)	1714 (2)	51 (1)
w3	9140 (2)	7590 (5)	1756 (2)	69 (1)
w4	7806 (2)	5039 (4)	1195 (2)	51 (1)
w5	5292 (2)	5967 (5)	1922 (2)	68 (1)
w6	4464 (2)	2966 (4)	2178 (2)	64 (1)
w7	10581 (2)	3917 (5)	3123 (2)	65 (1)

[a] Esd's in the least significant digits are given in parentheses. [b] For these values, the equivalent isotropic U is defined as $^1/_3$ of the trace of the U_{ij} tensor.

Final fractional atomic coordinates for all non-hydrogen atoms of **2** are listed in Table VI. Metric parameters relevant to the chelated cadmium ion, the partially aquated Sr^{2+} counterion, and the interionic interactions between these species are listed in Table VII (parts a, b, and c, respectively). Ligand structural parameters (Table VIII) have also been tabulated.

Results and Discussion

Structure of $Ca[Ca(EGTA)]\cdot(^{22}/_{3})H_2O$, 1. The asymmetric unit of the unit cell contains three $[Ca(EGTA)]^{2-}$ anions (anion a, Ca1; b, Ca2; c, Ca3); anion a, containing Ca1, is pictured in Figure 1a. Since the most commonly observed coordination number for calcium is eight,[41,42] it is not surprising that the $EGTA^{4-}$ ligand utilizes its full octadentate chelating capability in binding to Ca^{2+} in each of the $[Ca(EGTA)]^{2-}$ complexes. The ligand atoms about calcium in each of the three $[Ca(EGTA)]^{2-}$ complexes occupy the vertices of dodecahedra that are distorted by constraints associated with the chelate rings. A dodecahedron is formed by the orthogonal intersection of two equivalent trapezoids (each represented as BAAB, with AA being the shorter of the two parallel edges). In complex a, for example (see Figure 1b), one such trapezoid contains N2 and O6 (A sites) as well as O5 and O7 (B sites), while the second trapezoid contains O3 and N1 (A sites) together with O1 and O9 (B sites).

The three Ca^{2+} counterions are coordinated by water molecules and by the oxygen atoms of carboxylate groups that bridge be-

(41) Einspahr, H.; Bugg, C. E. in ref 3, Chapter 2, p 51.
(42) Einspahr, H.; Bugg, C. E. in *Calcium Binding Proteins and Calcium Function*; Wasserman, R. H.; Corradino, R. A.; Carafoli, E.; Kretsinger, R. H.; Maclennan, D. H.; Siegel, F. L., Eds.: Elsevier North-Holland: 1977, p 13.

Table VII. Metal–Ligand Distances (Å) and Angles (deg)[a] for $Sr[Cd(EGTA)]\cdot 7H_2O$

	a. Complex Ion		
Cd–N1	2.421 (4)	Cd–O5	2.574 (3)
Cd–N2	2.437 (3)	Cd–O6	2.585 (3)
Cd–O1	2.324 (3)	Cd–O7	2.420 (3)
Cd–O3	2.347 (3)	Cd–O9	2.325 (3)
N1–Cd–N2	148.0 (1)	O5–Cd–O6	63.5 (1)
N1–Cd–O1	71.0 (1)	N1–Cd–O7	91.8 (1)
N2–Cd–O1	83.4 (1)	N2–Cd–O7	68.7 (1)
N1–Cd–O3	70.6 (1)	O1–Cd–O7	90.0 (1)
N2–Cd–O3	127.3 (1)	O3–Cd–O7	81.2 (1)
O1–Cd–O3	140.2 (1)	O5–Cd–O7	159.9 (1)
N1–Cd–O5	71.7 (1)	O6–Cd–O7	136.3 (1)
N2–Cd–O5	131.1 (1)	N1–Cd–O9	139.5 (1)
O1–Cd–O5	95.1 (1)	N2–Cd–O9	71.7 (1)
O3–Cd–O5	82.5 (1)	O1–Cd–O9	143.9 (1)
N1–Cd–O6	118.1 (1)	O3–Cd–O9	75.4 (1)
N2–Cd–O6	69.6 (1)	O5–Cd–O9	82.8 (1)
O1–Cd–O6	72.8 (1)	O6–Cd–O9	74.2 (1)
O3–Cd–O6	136.6 (1)	O7–Cd–O9	104.2 (1)
	b. Counterion		
Sr–O9	2.764 (3)	Sr–w4	2.555 (3)
Sr–O10	2.696 (3)	Sr–O7a	2.995 (3)
Sr–w1	2.554 (5)	Sr–O8a	2.614 (3)
Sr–w2	2.734 (3)	Sr–O10a	2.559 (3)
Sr–w3	2.567 (4)		
O9–Sr–O10	47.6 (1)	w2–Sr–O7a	126.0 (1)
O9–Sr–w1	66.9 (1)	w3–Sr–O7a	64.7 (1)
O10–Sr–w1	80.9 (1)	w4–Sr–O7a	75.8 (1)
O9–Sr–w2	122.6 (1)	O9–Sr–O8a	74.2 (1)
O10–Sr–w2	92.2 (1)	O10–Sr–O8a	72.9 (1)
w1–Sr–w2	67.7 (1)	w1–Sr–O8a	141.2 (1)
O9–Sr–w3	148.3 (1)	w2–Sr–O8a	139.8 (1)
O10–Sr–w3	163.9 (1)	w3–Sr–O8a	110.5 (1)
w1–Sr–w3	102.7 (1)	w4–Sr–O8a	90.3 (1)
w2–Sr–w3	75.1 (1)	O7a–Sr–O8a	46.0 (1)
O9–Sr–w4	71.9 (1)	O9–Sr–O10a	119.9 (1)
O10–Sr–w4	119.4 (1)	O10–Sr–O10a	75.6 (1)
w1–Sr–w4	78.0 (1)	w1–Sr–O10a	128.9 (1)
w2–Sr–w4	128.6 (1)	w2–Sr–O10a	68.6 (1)
w3–Sr–w4	76.7 (1)	w3–Sr–O10a	90.4 (1)
O9–Sr–O7a	110.4 (1)	w4–Sr–O10a	152.6 (1)
O10–Sr–O7a	118.1 (1)	O7a–Sr–O10a	76.8 (1)
w1–Sr–O7a	153.0 (1)	O8a–Sr–O10a	71.6 (1)
	c. Interionic Angles		
Cd–O7–Sra	159.7 (1)	Sr–O9–C14	93.2 (2)
C12–O7–Sra	84.4 (2)	Sr–O10–C14	96.5 (2)
C12–O8–Sra	102.1 (2)	Sr–O10–Srb	104.4 (1)
Cd–O9–Sr	148.7 (1)	C14–O10–Srb	148.7 (2)

[a] Esd's in the least significant digits are given in parentheses.

tween the $[Ca(EGTA)]^{2-}$ complex anions and the partially aquated counterions. Such bridging in **1** is so extensive that no discrete $[Ca(EGTA)]^{2-}$ anions exist in the solid. Three modes of carboxylate bridging occur in **1** (see Figure 2a). A bridging carboxylate group is described as bidentate if both oxygen atoms are bound to a counterion (see, for example, O7 and O8 bridging to Ca5). A bridge that involves only the carboxylate oxygen atom that is *not* coordinated to Ca^{2+} of the $[Ca(EGTA)]^{2-}$ complex is described as unidentate(O′) (see, for example, O2 bridging to Ca6). Finally, a bridge that involves only the carboxylate oxygen atom that is coordinated to Ca^{2+} of the $[Ca(EGTA)]^{2-}$ complex is described as unidentate(O) (see, for example, O29 bridging to Ca6). All three bridging modes seen in **1** have been previously observed,[42,43] but never before in the same material.

Complex anions a and b exhibit identical bridging patterns and are related by an approximate noncrystallographic twofold axis passing through Ca5. Three of the carboxylate groups in each

(43) Ancillotti, F.; Boschi, G.; Perego, G.; Zazzetta, A. *J. Chem. Soc., Dalton Trans.* 1977, 901.

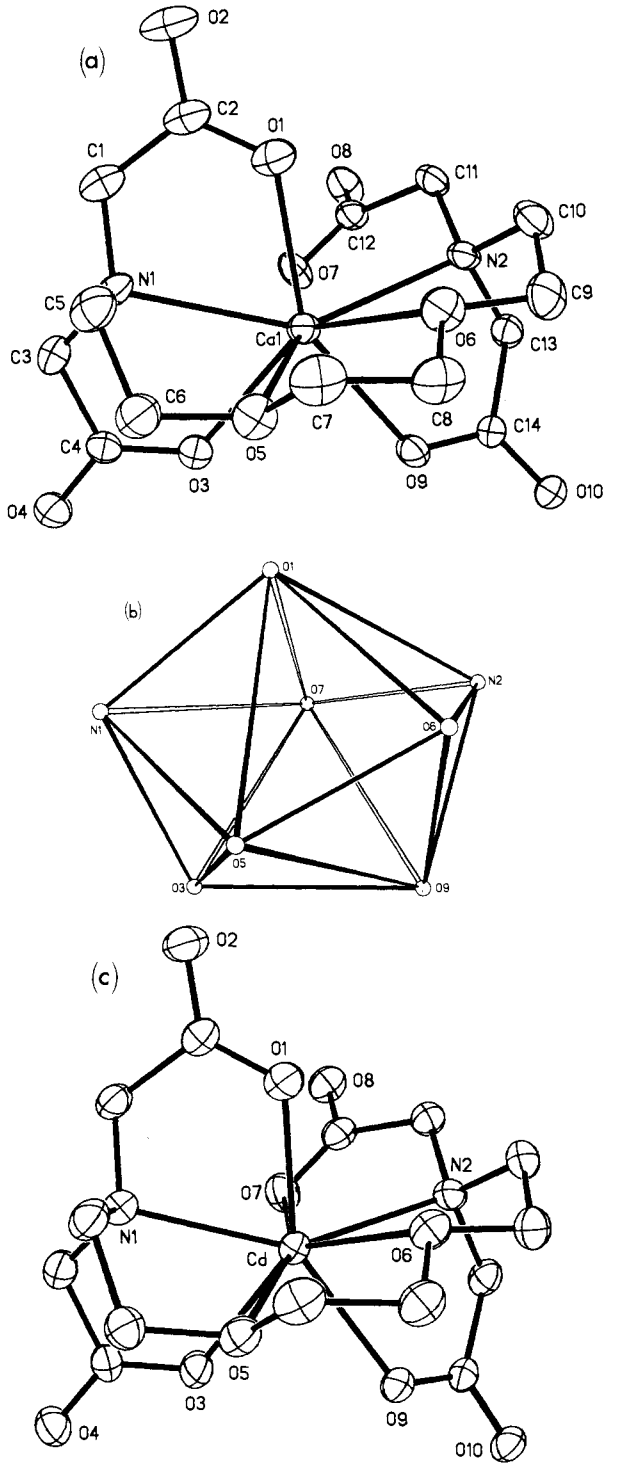

Figure 1. (a) Thermal ellipsoid plot (40%) of the $[Ca(EGTA)]^{2-}$ complex anion involving Ca1. The numbering scheme for the complex anions involving Ca2 and Ca3 may be derived as follows: for Cx, $x = 14(n-1) + a$; for Ox, $x = 10(n-1) + a$; for Nx, $x = 2(n-1) + a$; n = complex anion number, a = atom number in the complex involving Ca1. (b) The dodecahedron of ligand atoms about Ca1. (c) Thermal ellipsoid plot (40%) of $[Cd(EGTA)]^{2-}$. The numbering scheme for the ligand is identical with that employed in the $[Ca(EGTA)]^{2-}$ anion in Figure 1a.

of these $[Ca(EGTA)]^{2-}$ anions act as external donors, bridging to the Ca^{2+} counterions (Ca4, Ca5, and Ca6). Two of these three carboxylate groups bridge in a bidentate fashion (O7/O8 and O9/O10 in a, O17/O18 and O19/O20 in b), while the remaining group (O1/O2 in a, O11/O12 in b) bridges in a unidentate(O′) fashion. In anion c, only two of the four carboxylate groups bridge to counterions. Both of these groups (O23/O24 and O29/O30) bridge in a unidentate(O) manner; anion c thus functions as a bidentate ligand with respect to Ca6 (see Figure 2a).

Table VIII. Chelate Ring[a] Bonding Parameters[b] for $Sr[Cd(EGTA)]\cdot 7H_2O$

Glycinate Rings

	C–C′	C′–N	C–O	C–O′	C–C′–N
G1	1.533 (6)	1.472 (5)	1.267 (5)	1.234 (5)	112.8 (3)
G2	1.496 (6)	1.472 (5)	1.252 (5)	1.251 (5)	114.2 (4)
G3	1.526 (6)	1.465 (5)	1.250 (5)	1.258 (5)	113.6 (3)
G4	1.514 (6)	1.467 (5)	1.257 (5)	1.256 (5)	115.2 (3)
	O–C–O′	C′–C–O	C′–C–O′	Cd–N–C′	Cd–O–C
G1	125.5 (4)	117.9 (3)	116.6 (4)	104.4 (2)	116.9 (2)
G2	123.8 (4)	118.5 (3)	117.6 (4)	110.8 (2)	120.5 (3)
G3	124.5 (4)	119.0 (4)	116.5 (4)	107.4 (2)	115.3 (2)
G4	122.5 (3)	119.5 (3)	118.0 (3)	105.1 (2)	116.5 (2)

Amino Ether Rings

	C–C′	C–N	C′–O	C–C′–O	C′–C–N
A1	1.509 (6)	1.485 (5)	1.433 (6)	110.7 (4)	111.9 (3)
A2	1.508 (6)	1.481 (5)	1.427 (5)	107.3 (3)	113.4 (3)
	C″–N–C†	C–N–C″	C–N–C†	Cd–N–C	Cd–O–C′
A1	112.1 (3)	108.7 (3)	111.7 (3)	108.8 (2)	108.7 (2)
A2	111.1 (3)	110.0 (3)	111.5 (3)	111.5 (2)	111.0 (2)

Diether Ring

	C–C′	C′–O′	C–O	C′–C–O	C–C′–O′
E1	1.498 (7)	1.419 (5)	1.437 (5)	107.4 (3)	106.7 (3)
	C′–O′–C†	C″–O–C	Cd–O–C	Cd–O′–C′	
E1	113.2 (3)	112.9 (3)	115.3 (2)	116.4 (2)	

[a] Chelate ring designations are described in footnote a of Table V. [b] Bond lengths are given in Å and bond angles in deg. Esd's in the least significant digits are given in parentheses.

Of the three Ca^{2+} counterions, two (Ca4 and Ca5) are eight-coordinate and exhibit similar ligand arrays. Each of these ions is coordinated by two bidentate bridging carboxylate groups from $[Ca(EGTA)]^{2-}$ anions (O7/O8 and O17/O18 for Ca5, for example) and by oxygen atoms of four water molecules. The coordination spheres about Ca4 and Ca5 are distorted dodecahedra. Significant differences exist in the arrangements of ligand atoms in those coordination spheres, however. In the two trapezoids of the dodecahedron about Ca4, oxygen atoms of bidentate carboxylate groups occupy A sites, while oxygen atoms of water molecules occupy B sites. About Ca5, on the other hand, oxygen atoms of bidentate carboxylate groups occupy an A and a B site in each trapezoid.

The third counterion, Ca6, is only seven-coordinate. Among the ligands about Ca6 are three water molecules and the oxygen atoms of four bridging carboxylate groups, two of the unidentate(O′) type and two of the unidentate(O) type. The ligand atoms bound to Ca6 occupy the vertices of a distorted monocapped trigonal prism, with triangular faces outlined by O29, O23, and w10 and by O2, O12, and w9. The oxygen atom of water molecule w11 caps the rectangular w10–O23–O12–w9 face (see Figure 2a). The lower coordination number for Ca6 may be due to greater steric requirements of unidentate bridging carboxylate groups.

The $[Ca(EGTA)]^{2-}$ anions and the partially aquated Ca^{2+} counterions are linked by the carboxylate bridges into polymeric chains, which are propagated parallel to the *bc* plane. In addition, hydrogen bonds connect carboxylate groups and coordinated water molecules to occluded solvent water molecules. Every carboxylate oxygen atom in **1** is involved in an interaction with a metal ion or a water molecule. Anion c bridges to only one cation (Ca6) and therefore functions as a side group on the polymer chain. These side groups extend from the chain in the *a* direction and stitch the chains together by hydrogen bonding to water molecules coordinated to cations on adjacent chains. The extensive hydrogen bonding network is an important factor in the stability of crystals of **1**.

The Ca–O(carboxylate) bond distances in **1** are a function of the bridging nature of the carboxylate group. Ca–O(carboxylate)

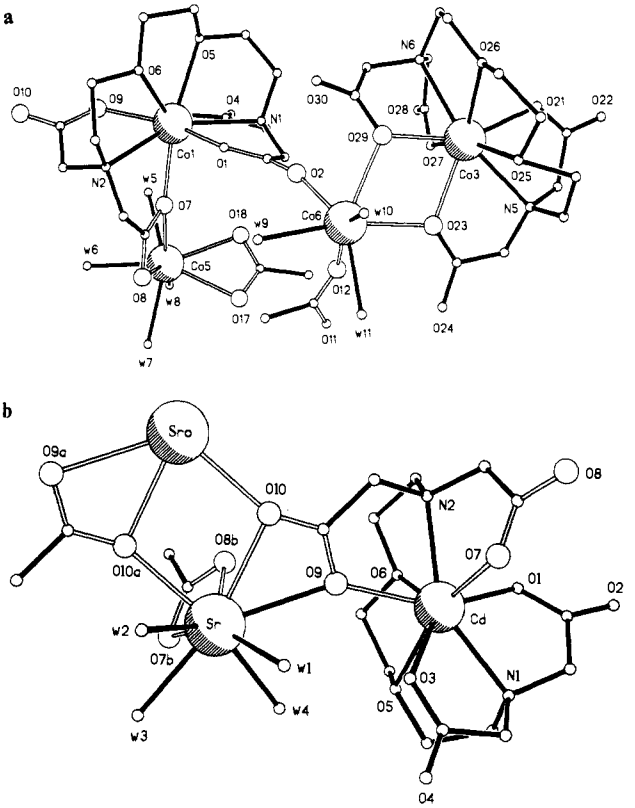

Figure 2. (a) Ball and stick plot depicting all the unique interionic interactions occurring in **1** (see text). In the two complex ions illustrated, all oxygen atoms that are involved in bridging interactions are enlarged. Hollowed bonds highlight the bridging pathways between the $[Ca(EGTA)]^{2-}$ anions and the calcium counterions. (b) Ball and stick plot depicting all the unique interionic interactions occurring in **2**. Conventions used are the same as in Figure 2a.

bonds in the $[Ca(EGTA)]^{2-}$ anions are, with the exception of those involving unidentate(O′) bridging groups, shorter than Ca–O(carboxylate) bonds for the Ca^{2+} counterions. For example, the bidentate bridging carboxylate group O7/O8 binds more strongly to Ca1 (Ca1–O7 = 2.404 (4) Å) than to the Ca5 counterion (Ca5–O7 = 2.526 (4), Ca5–O8 = 2.485 (4) Å). In all of the bidentate bridging groups, the oxygen atom that is not bound to Ca^{2+} of a $[Ca(EGTA)]^{2-}$ anion binds to the counterion at a shorter distance than does the oxygen atom that is bound to both Ca^{2+} ions.

Unidentate(O′) bridging carboxylate groups do not exhibit as regular a pattern of Ca–O bond lengths. One unidentate(O′) bridging group (O11/O12) exhibits a shorter bond to the Ca^{2+} ion of anion b (Ca2–O11 = 2.347 (4) Å) than to the associated Ca^{2+} counterion (Ca6–O12 = 2.381 (4) Å). The reverse is true (Ca1–O1 = 2.375 (4), Ca6–O2 = 2.325 (5) Å) for the other such group. Similar bond length vs. bridge type patterns occurred in bidentate and unidentate(O′) bridges in $Ca[Ca(EDTA)]\cdot 7H_2O$.[44]

The two unidentate(O) bridges form a planar Ca_2O_4 unit. The bridge involving O23 is symmetric (Ca3–O23 = 2.412 (4), Ca6–O23 = 2.407 (5) Å), while the bridge involving O29 is nonsymmetric, with O29 binding at a shorter distance to the chelated Ca^{2+} ion (Ca3–O29 = 2.397 (5) Å) than to the Ca^{2+} counterion (Ca6–O29 = 2.473 (4) Å). Comparison with other Ca–O bond distances[41,42] reveals that all Ca–O(carboxylate) distances in **1** (2.325 (5)–2.542 (4), average = 2.38 (2) Å) fall within the normal range for seven- and eight-coordinate Ca^{2+} ions. In addition, $Ca–OH_2$ distances in **1** span a range (2.386 (4)–2.485 (5) Å) typical of seven- and eight-coordinate aquated Ca^{2+} complexes.

The question of whether the $EGTA^{4-}$ ligand utilizes its ether oxygen atoms in coordinating to various metal ions, including

(44) Barnett, B. L.; Uchtman, V. A. *Inorg. Chem.* **1974**, *18*, 2674.

calcium, has been disputed.[45-47] In **1**, however, the ether oxygen atoms in all three crystallographically independent $[Ca(EGTA)]^{2-}$ complexes are coordinated ($Ca-O(ether)_{av}$ = 2.50 (3) Å). Given the chelating nature of $EGTA^{4-}$, it seems likely that the ether oxygen atoms remain bound in solution. The abnormally short Ca3–O25 distance was omitted in calculating the average given above; this distance has clearly been influenced by the disorder present in the chelate ring containing C34. All of the Ca–O(ether) distances (except for Ca3–O25) in **1** fall within the range observed previously for Ca–O(ether) bond lengths. For example, in nine-coordinate $[Ca(2.2.2)Br]^+$ (2.2.2 = 4,7,13,16,21,24-hexaoxa-1,10-diazabicyclo[8.8.8]hexaeicosane),[48] Ca–O(ether) distances span a range (2.487 (7)–2.551 (7) Å) almost identical with that in **1** (2.473 (4)–2.550 (4) Å).

The Ca–N bonds in **1** (Ca–N = 2.567 (5)–2.617 (5) Å) are longer than any of the Ca–O bonds. However, the Ca–N bonds in anions a and b (Ca–N(av) = 2.609 (7) Å) are shorter than the Ca–N bonds in the eight-coordinate $EDTA^{4-}$ complex (Ca–N = 2.623 (7), 2.711 (8) Å) and the octahedral NTA^{3-} (NTA^{3-} = nitrilotriacetate) complex (Ca–N = 2.629 (2) Å).[44] The Ca–N bonds in complex c (Ca–N = 2.575 (6), 2.567 (5) Å) are shorter than the Ca–N bonds in complexes a and b, as a result of the simultaneous involvement of O23 and O29 in unidentate(O) bridges. As a result of this bridging arrangement, the O23···O29 distance (3.190 (6) Å) in complex c is significantly shorter than the corresponding distances (O3···O9 = 3.279 (6), O13···O19 = 3.298 (6) Å) in complexes a and b. Thus, binding of O23 and O29 to Ca6 appears to act to tighten the $EGTA^{4-}$ ligand about Ca3.

The two aminodiacetate termini bind to Ca^{2+} very differently. At one end of the $EGTA^{4-}$ ligand in anion a, Ca1 is approximately coplanar with the coordinating atoms N1, O1, and O3. In contrast, Ca1 does not lie near the plane formed by N2, O7, and O9 at the other end of the ligand. These meridional (N1, O1, O3) and bent (N2, O7, O9) arrangements of the termini persist in all three of the crystallographically independent complex anions in **1**.

The conformations of the five-membered chelate rings in all three of the $[Ca(EGTA)]^{2-}$ anions have been analyzed by the method used to assess conformations in steroid ring systems[49] and in other polyamino–polycarboxylate complexes.[50] The values of the asymmetry parameters for the glycinate chelate rings, the amino ether chelate rings, and the diether chelate rings are all similar to values reported for other aminocarboxylate complexes.

Structure of $Sr[Cd(EGTA)]\cdot 7H_2O$ (2). The structure of the $[Cd(EGTA)]^{2-}$ anion in **2** is similar to that of the $[Ca(EGTA)]^{2-}$ anions of **1**, as can be seen by comparison of Figure 1 (parts c and a). The $EGTA^{4-}$ ligand is octadentate in coordinating to Cd(II), despite cadmium's slightly smaller ionic radius (for eight-coordinate metal ions, $r_{Ca(II)}$ = 1.12 Å, $r_{Cd(II)}$ = 1.10 Å).[51] The coordination geometry about Cd^{2+} remains approximately dodecahedral.

Five of the nine oxygen atoms surrounding the Sr^{2+} counterion come from bridging carboxylate groups, and the remaining four come from water molecules. Two of the four carboxylate groups of the $[Cd(EGTA)]^{2-}$ anion are involved in bridging interactions. One carboxylate group (O9/O10) functions simultaneously as a bidentate and a unidentate(O′) donor to two symmetry-related Sr^{2+} ions (see Figure 2b). The other bridging carboxylate group (O7/O8) acts solely as a unidentate(O′) donor. The nine ligand atoms about Sr^{2+} occupy the vertices of a slightly twisted tricapped trigonal prism, with triangular faces composed of O10, O8a, and O10a as well as w3, w1, and w4. The prism is capped by atoms O9, w2, and O7a.

The bridging bond lengths to Sr^{2+} span a large range of values (2.559 (3)–2.995 (3) Å). The Sr–O7a distance (2.995 (3) Å) is more than 0.2 Å greater than any other Sr–O(carboxylate) distance in **2** and must represent an extremely weak interaction. Despite the fact that O10 is involved in both a bidentate and a unidentate(O′) bridge, the unidentate(O′) bridge exhibits the shortest Sr–O(carboxylate) distance (Sr–O10a = 2.559 (3) Å). In the bidentate bridges, the oxygen atom that is simultaneously bound to Cd^{2+} exhibits a longer bond to Sr^{2+} (Sr–O7a = 2.995 (3), Sr–O8a = 2.614 (3), Sr–O9 = 2.764 (3), Sr–O10 = 2.696 (3) Å). The average Sr–O(carboxylate) distance in $Mg[Sr(EGTA)(OH_2)]\cdot 7H_2O$[52] is 2.67 (6) Å, with a range of 2.588 (4)–2.722 (5) Å. This range agrees well with the range of Sr–O(carboxylate) distances for **2**, with the exception of the very long bond to O7a. Three of the $Sr-OH_2$ distances in **2** are equal within experimental error ($Sr-OH_2(av)$ = 2.559 (7) Å), while one is significantly longer (Sr–w2 = 2.734 (3) Å).

Like **1**, **2** is held together in the solid state by carboxylate bridges between metal ions and by hydrogen bonds. Three occluded water molecules participate in hydrogen bonding with carboxylate groups and coordinated water molecules to connect the polymeric cation/anion chains.

In the $[Cd(EGTA)]^{2-}$ anion, one Cd–O(carboxylate) bond length (Cd–O7 = 2.420 (3) Å) is longer than the other three (Cd–O1 = 2.324 (3), Cd–O3 = 2.347 (3), Cd–O9 = 2.325 (3) Å). The O3···O7 distance (3.101 (6) Å) is 0.19 Å shorter than the corresponding distances in the relatively unconstrained a and b chelates in **1** (O3···O7(av) = 3.29 (1) Å). O3 and O9 also approach each other more closely in **2** (by 0.18 Å) than in the a and b chelates in **1**. If O7 were bound to cadmium(II) at a normal distance, it would force O3 and O7 into even closer proximity. These changes in intrachelate contact distances, together with the long Cd–O7 bond, suggest that the $EGTA^{4}$ ligand fits less well about the slightly smaller Cd^{2+} ion than it does about the Ca^{2+} ion.

The Cd–O(carboxylate) distances in **2** (Cd–O(carb,av) = 2.35 (5) Å) are similar to those in the seven-coordinate $[Cd(EDTA)(OH_2)]^{2-}$ anion (Cd–O(carb,av) = 2.39 (5) Å),[53] despite the difference in coordination number. They are also similar to the Ca–O(carboxylate) distances in the $[Ca(EGTA)]^{2-}$ anions of **1** (Ca–O(carb,av) = 2.38 (2) Å).

Differences between **1** and **2** surface when metal–N and metal–O(ether) bond lengths are compared. The Cd–N distances (Cd–N(av) = 2.43 (1) Å) in **2** are much shorter than the Ca–N distances (Ca–N(av) = 2.609 (7) Å) in the a and b chelates in **1**. The Cd–N distances in **2** are slightly longer than those in $[Cd(EDTA)(OH_2)]^{2-}$ (Cd–N = 2.382 (9), 2.414 (7) Å).[53]

In contrast, Cd–O(ether) bonds are longer than Ca–O(ether) distances (Cd–O(ether,av) = 2.580 (8), Ca–O(ether,av) = 2.50 (4) Å in anions a and b of **1**). For the seven-coordinate cadmium ion in $[Cd(ODA)]\cdot 3H_2O$ (ODA = oxydiacetate),[54] Cd–O(ether) = 2.49 (1) Å; for six- and seven-coordinate cadmium ions in $Cd_2(TGM)Cl_4$[55] (TGM = tetraethylene glycol dimethyl ether), the Cd–O(ether) distances for ether oxygen atoms not involved in bridging ranged from 2.41 (1)–2.52 (1) Å (Cd–O(av) = 2.46 (5) Å). The differences between the Cd–O bond lengths in **2** and these literature values are expected, given the differences in coordination numbers.[51]

Values of the bond angles about the Ca^{2+} and Cd^{2+} ions differ significantly (see Tables IV and VII). In amino ether rings, O–Ca–N < O–Cd–N, Ca–O–C′ > Cd–O–C′, and Cd–N–C > Ca–N–C. These differences are as expected, given that the shortening of the Cd–N bonds (compared to Ca–N) is of greater magnitude than the lengthening of the Cd–O(ether) bonds

(45) Bryson, A.; Nancollas, G. H. *Chem. Ind.* **1965**, 645.
(46) Mirti, P.; Gennaro, M. C. *J. Inorg. Nucl. Chem.* **1981**, *43*, 3221.
(47) Mirti, P. *J. Inorg. Nucl. Chem.* **1979**, *41*, 323.
(48) Metz, P. B.; Moras, D.; Weiss, R. *Acta Crystallogr., Sect. B: Struct. Crystallogr. Cryst. Chem.* **1973**, *B29*, 1377.
(49) Duax, W. L.; Norton, D. A. *Atlas of Steroid Structure*; Vol 1, IFI/Plenum: New York, 1975; p 17.
(50) Stezowski, J. J.; Hoard, J. L. *Isr. J. Chem.* **1984**, *24*, 323.
(51) Shannon, R. D. *Acta Crystallogr., Sect. A: Cryst. Phys., Diffr., Theor. Gen. Crystallogr.* **1976**, *A32*, 751.
(52) Schauer, C. K.; Anderson, O. P., unpublished results.
(53) Solans, X.; Gali, S.; Font-Altaba, M.; Oliva, J.; Herrera, J. *Acta Crystallogr., Sect. B: Struct. Sci.* **1983**, *B39*, 438.
(54) Boman, C.-E. *Acta Crystallogr. Sect. B: Struct. Crystallogr. Cryst. Chem.* **1977**, *B33*, 838.
(55) Iwamoto, R.; Wakano, H. *J. Am. Chem. Soc.* **1976**, *98*, 3764.

(compared to Ca–O(ether)). The shorter Cd–N bonds also dictate the angular differences seen in the glycinate rings: Ca–O–C′ > Cd–O–C′, Ca–N–C′ > Cd–N–C′, and N–Cd–O > N–Ca–O.

^{1}H NMR Spectra. The ^{1}H NMR spectra of EGTA^{4-} and several of its metal complexes have been described previously.[45-47] Splitting patterns in ^{1}H NMR spectra can allow qualitative judgments about bond labilities for a chelate in solution,[56-58] but such analyses require that frequency differences between theoretically inequivalent protons be sufficiently large to observe predicted splitting patterns.[36] This requirement made interpretation of the 60-MHz room temperature NMR spectrum of [Ca(EGTA)]$^{2-}$ difficult.[46] At 200 MHz, [Ca(EGTA)]$^{2-}$ exhibits an AB quartet for the acetate protons, a singlet for the protons of the diether ring, and two broadened triplets for the protons of the amino ether rings (see Experimental Section). A similar splitting pattern is seen for [Cd(EGTA)]$^{2-}$,[36] but in that case the AB pattern is further split by the presence of ^{111}Cd (12.75%, $I = {}^1/_2$) and ^{113}Cd (12.26%, $I = {}^1/_2$).

The AB and ABX patterns for the acetate protons of the Ca^{2+} and Cd^{2+} complexes imply that inversion at nitrogen is not occurring on the NMR time scale at room temperature for either of the complexes. This, in turn, implies that the Ca–N and Cd–N bonds are not labile, since such lability (with rapid inversion) would result in exchange of the diastereotopic A and B protons. The single AB quartet for the acetate protons implies that a rapid (on the NMR time scale) bond dissociation and rearrangement process results in higher average symmetry (C_{2v}) for the complexes in solution than that observed in the solid state (C_1). This must be accomplished by breaking of metal–O(carboxylate) bonds, allowing interconversion between centrosymmetrically related complex anions.

The acetate AB pattern for [Ca(EGTA)]$^{2-}$ coalesces to a singlet as the temperature is raised. This implies that Ca–N bond breaking, which allows inversion at nitrogen to occur, becomes rapid on the NMR time scale at elevated temperature. Given the large difference in M–N bond distances for the Ca^{2+} and Cd^{2+} complexes, a difference in the activation parameters for nitrogen atom dissociation would be expected. The failure of the ABX pattern for [Cd(EGTA)]$^{2-}$ to coalesce completely, even when the solution is heated in a sealed tube to 120 °C, is consistent with this expectation.

^{113}Cd Solution and Solid-State NMR Spectra. Cd^{2+} has been used extensively in biological systems as an NMR spectroscopic replacement for Ca^{2+}, Mg^{2+}, and Zn^{2+} ions.[23,24] ^{113}Cd is a sensitive, relatively abundant nucleus with a large chemical shift range (≈900 ppm). The ^{113}Cd NMR spectra of cadmium-substituted calcium-binding proteins exhibit a chemical shift range of −85 to −130 ppm (relative to 0.1 M $Cd(ClO_4)_2$(aqueous)). The only Cd^{2+} complex that exhibits a solution chemical shift value that highly shielded involves a macrocyclic ligand containing six ether oxygen atoms and four pendant carboxylate groups; the ^{113}Cd resonance for that complex occurs at −130 ppm.[59]

In solution, partial substitution by solvent results in a ^{113}Cd chemical shift value that is the average for all of the variously substituted complexes; this makes it difficult for a complex in solution to exhibit a chemical shift value in the calcium-binding protein range, since the proteins are not subject to such effects. As a result, solid-state ^{113}Cd NMR spectra, even of species such as $Cd(NO_3)_2{\cdot}4H_2O$ and $Cd(OAc)_2{\cdot}2H_2O$,[60-62] are more likely to exhibit resonances in the calcium-binding protein chemical shift range. Recently, single-crystal ^{113}Cd NMR studies[63,64] have been used to identify the interactions that determine the components of the shielding tensor. In the compounds studied thus far, the most highly shielded components of the tensor are oriented perpendicular to long Cd–O bonds.

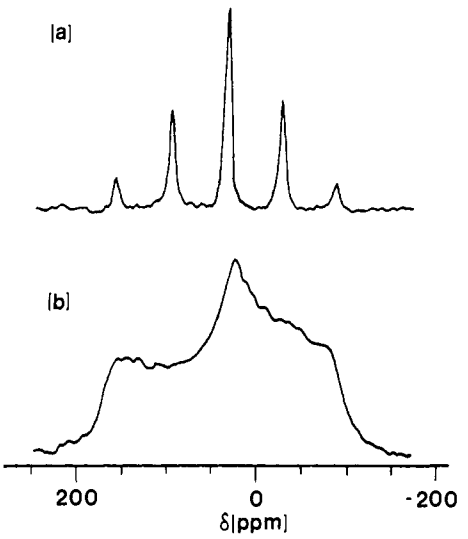

Figure 3. (a) Magic angle spinning ^{113}Cd spectrum of a powder ground from crystals of $Sr[Cd(EGTA)]{\cdot}7H_2O$. The spinning sidebands are modulated at the rotor speed. $\delta(^{113}Cd) = +36$ ppm. (b) Nonspinning powder pattern for **2**. The principal components of the shielding tensor are $\sigma_{11} = 159$, $\sigma_{22} = 29$, $\sigma_{33} = -81$ ppm.

While the present work was in progress, the ^{113}Cd NMR spectrum of [Cd(EGTA)]$^{2-}$ in solution was reported.[65] In solution, the ^{113}Cd resonance for [Cd(EGTA)]$^{2-}$ is 15 ppm deshielded from the 0.1 M $Cd(ClO_4)_2$ standard. The Cd^{2+}–EDTA complex exhibits a ^{113}Cd chemical shift of +85 ppm[66] relative to the same standard; the more shielded Cd^{2+}–EGTA resonance, relative to that for the Cd^{2+}–EDTA complex, apparently results from replacement of a single water molecule by two ether oxygen atoms. The presence of the nitrogen atoms (known to shift ^{113}Cd resonances toward a less shielded position) in **2** means that the [Cd(EGTA)]$^{2-}$ complex cannot be expected to reproduce the ^{113}Cd chemical shifts characteristic of cadmium-substituted calcium-binding proteins, despite the presence of six oxygen atoms in the metal's primary coordination sphere.

The ^{113}Cd spectra obtained from powdered **2** are shown in Figure 3, parts a (magic angle spinning) and b (nonspinning). These spectra yield a ^{113}Cd chemical shift value (+36 ppm) that is free of the influence of the ligand substitution processes that affect the solution value. The metal–ligand bond-breaking processes which occur in solution (see above) must temporarily replace carboxylate oxygen atoms by water molecules; this was expected to result in a more deshielded chemical shift value for the ^{113}Cd resonance in solution, compared to that for the complex in the solid state. Surprisingly, the solid-state resonance occurs at a less highly shielded position (by 21 ppm) than does the solution resonance. The chemical shift sensitivity of ^{113}Cd is such that changes in the ligand binding induced by the bridging interactions to Sr^{2+} counterions may cause this unexpected chemical shift behavior.

The nonspinning pattern for **2** is consistent with its low symmetry. Three distinct elements of the shielding tensor are observed ($\sigma_{11} = 159$, $\sigma_{22} = 29$, $\sigma_{33} = -81$ ppm); the chemical shift anisotropy spans 240 ppm. Only the value of the most highly shielded component lies in the range of chemical shifts exhibited by cadmium-substituted calcium-binding proteins. This component of the shielding tensor is probably roughly perpendicular to the long Cd–O(ether) bonds.

(56) Day, R. J.; Reilley, C. N. *Anal. Chem.* **1964**, *36*, 1073.
(57) Day, R. J.; Reilley, C. N. *Anal. Chem.* **1965**, *37*, 1326.
(58) Gennaro, M. C.; Mirti, P.; Casaline, C. *Polyhedron* **1983**, *1*, 13.
(59) Keller, A. D.; Drakenberg, T.; Briggs, R. W.; Armitage, I. M. *Inorg. Chem.* **1985**, *24*, 1170.
(60) Murphy, P. D.; Gerstein, B. C. *J. Am. Chem. Soc.* **1981**, *103*, 3282.
(61) Cheung, T. T. P.; Worthington, L. E.; DuBois Murphy, P.; Gerstein, B. C. *J. Magn. Reson.* **1980**, *41*, 158.
(62) Mennitt, P. G.; Shatlock, M. P.; Bartuska, V. J.; Maciel, G. E. *J. Phys. Chem.* **1981**, *85*, 2087.
(63) Honkonen, R. S.; Doty, R. D.; Ellis, P. D. *J. Am. Chem. Soc.* **1983**, *105*, 4163.
(64) Honkonen, R. S.; Ellis, P. D. *J. Am. Chem. Soc.* **1984**, *106*, 5488.
(65) Live, D.; Armitage, I. M.; Dalgarno, D. C.; Cowburn, D. *J. Am. Chem. Soc.* **1985**, *107*, 1775.
(66) Jensen, C. F.; Deshmukh, S.; Jakobsen, H. J.; Inners, R. R.; Ellis, P. D. *J. Am. Chem. Soc.* **1981**, *103*, 3659.

Implications for Ca^{2+}-Binding Proteins. Since Cd–O(carboxylate) distances proved to be very similar to Ca–O(carboxylate) distances in the $EGTA^{4-}$ complexes and coordination numbers in the two complexes were identical, one infers that the Cd^{2+} ion is a good choice as a spectroscopic probe for calcium-binding site structure. However, it should be noted that calcium-selective proteins utilize neutral oxygen donors (carbonyl oxygen atoms and hydroxyl groups) as well as anionic carboxylate donors to bind Ca^{2+}. Substitution of Cd^{2+} for Ca^{2+} at a protein metal-binding site results, as noted above, in observation of a highly shielded ^{113}Cd resonance. Since the Cd^{2+} ion has shown a distinctly lower affinity for neutral oxygen donors than Ca^{2+} in the present study, and since long Cd–O distances are thought to be associated with highly shielded chemical shift values from single-crystal NMR studies, the low affinity of Cd^{2+} for neutral oxygen donors, rather than intrinsic site structure, may be responsible for the highly shielded chemical shift values characteristic of the cadmium-substituted proteins.

Acknowledgment. The Nicolet R3m/E X-ray diffractometer and computing system at Colorado State University was purchased with funds provided by the National Science Foundation. Solid-state ^{113}Cd NMR spectra were recorded in the Colorado State University Regional NMR Center, funded by the National Science Foundation. We thank Dr. Bruce Hawkins for obtaining the ^{113}Cd solid-state NMR spectra.

Supplementary Material Available: Table S-I—chelate ring conformational parameters for **1**, Table S-II—inter-ring torsion angles for **1**, Table S-III—anisotropic thermal parameters for **1**, Table S-IV—calculated hydrogen atom coordinates for **1**, Table S-VI—chelate ring conformational parameters for **2**, Table VII—inter-ring torsion angles for **2**, Table S-VIII—anisotropic thermal parameters for **2**, Table S-IX—calculated hydrogen atom coordinates for **2**, Table S-XI—selected least-squares planes for **1**, Table S-XII—hydrogen bonding distances in **1**, Table S-XIII—selected least-squares planes for **2**, Table S-XIV—hydrogen bonding distances in **2**, Figure S-1—view of the unit cell of **1**, and Figure S-2—view of the unit cell of **2** (26 pages); Tables S-V and S-X—observed and calculated structure factors, ×10, for **1** and **2**, respectively (86 pages). Ordering information is given on any current masthead page.

Crystal and Molecular Structure of the Charge-Transfer Salt of Decamethylcobaltocene and Tetracyanoethylene (2:1): $\{[Co(C_5Me_5)_2]^+\}_2[(NC)_2CC(CN)_2]^{2-}$. The Electronic Structures and Spectra of $[TCNE]^n$ (n = 0, 1–, 2–)

David A. Dixon* and Joel S. Miller*

Contribution No. 4175 from the Central Research and Development Department, E. I. du Pont de Nemours & Co., Experimental Station E328, Wilmington, Delaware 19898.
Received August 15, 1986

Abstract: The reaction of decamethylcobaltocene, $Co(C_5Me_5)_2$, and tetracyanoethylene, TCNE, leads to the isolation of two phases of 1:1 and 2:1 composition. The crystal and molecular structure of the 2:1 substance has been determined by single-crystal X-ray analysis at −50 °C. The red-orange 2:1 complex crystallizes as the acetonitrile solvate in the triclinic $P\bar{1}$ space group (No. 2) [a = 10.579 (6) Å, b = 14.142 (7) Å, c = 15.939 (5) Å, α = 114.73 (3)°, β = 94.40 (4)°, γ = 91.48 (4)°, V = 2155 (4) Å^3, and Z = 2]. The unit cell is comprised of two independent $[Co(C_5Me_5)_2]^+$ cations, an anion, and a MeCN solvent molecule. The final weighted R_w was 0.083. The C_5 Co^{III} cation is ordered and is essentially structurally equivalent to the isoelectronic $Fe^{II}(C_5Me_5)_2$; however, the average C–C and Co^{III}–C_5 ring distances are ~0.04 Å shorter than the analogous distances observed for $[Fe^{III}(C_5Me_5)_2]^+$. The dianion structure possesses approximate D_{2d} local symmetry with C—C and average C—CN and C≡N distances of 1.49 (2), 1.392 (8), and 1.166 (3) Å, respectively. The $[C(CN)_2]^-$ groups have an 87.1 ± 0.3° dihedral angle. For the $[TCNE]^n$ series for n = 0 the C–CN distance is greater than the C–C distance; for n = 2– the converse is true, and for n = 1– the distances are comparable. The $[TCNE]^n$ (n = 0, 1–, 2–) moieties have been characterized by infrared, Raman, and UV–vis spectroscopic techniques. The electronic absorption spectra of $[TCNE]^{\cdot-}$ exhibits a band (λ_{max} ≈ 23 375 cm^{-1}; ϵ ~ 8425 M^{-1} cm^{-1}) with a progression of 17 vibrational transitions (~550 cm^{-1}) tentatively assigned to coupling of the excited-state C–CN bend to the Π–Π^* transition. TCNE exhibits a $\Pi \rightarrow \Pi^*$ transition at 38 300 cm^{-1} with four vibrational overtones (~1200 cm^{-1}) tentatively assigned to coupling to the ν(C=C) vibration. The electronic structures of $[TCNE]^n$ (n = 0, 1–, 2–) have been calculated by ab initio molecular orbital theory with the STO-3G basis set and additionally for n = 0 and 2– with a double-ζ basis set augmented by a set of d polarization functions at the ethylene sp^2 carbons. The latter method gives results that are in good agreement with those obtained with ab initio STO-3G basis sets. The geometries were determined with both basis sets. The force fields were determined with both basis sets, and the frequencies are compared to the experimental values. These results confirm the D_{2h} and D_{2d} structures of $[TCNE]^{\cdot-}$ and $[TCNE]^{2-}$, respectively. Charge and spin distributions are presented and are discussed in terms of classical resonance structures.

Since our observation of molecular metamagnetism[1,2] and ferromagnetism[2,3] for the 1:1 TCNQ and TCNE (TCNQ = 7,7,8,8-tetracyano-*p*-quinodimethane; TCNE = tetracyanoethylene) salts of decamethylferrocene, respectively, we have sought to understand the structure-function relationship of metallocenium salts of strong acceptor anions with the particular focus on understanding the microscopic basis for cooperative magnetic phenomena in molecular materials. With our recent discovery of the means to stabilize dianionic acceptors[4] enabling their structural and spectroscopic characterization, we have prepared $\{[Co(C_5Me_5)_2]^+\}_2[TCNE]^{2-}$ and studied its physical properties. We are particularly interested in this compound as it allows comparison with other percyano anions and also provides a closed-shell model compound with which to compare other cyano

(1) Candela, G. A.; Swartzendruber, L. J.; Miller, J. S.; Rice, M. J. *J. Am. Chem. Soc.* **1979**, *101*, 2755.
(2) Miller, J. S.; Epstein, A. J.; Reiff, W. M. *Isr. J. Chem.*, in press.
(3) (a) Miller, J. S.; Calabrese, J. C.; Epstein, A. J.; Bigelow, R. W.; Zhang, J. H.; Reiff, W. M. *J. Chem. Soc., Chem. Commun.* **1986**, 1026. (b) Miller, J. S.; Calabrese, J. C.; Chittapeddi, S. R.; Zhang, J. H.; Reiff, W. H.; Epstein, A. J. *J. Am. Chem. Soc.* **1987**, *109*, 769.
(4) Miller, J. S.; Dixon, D. A. *Science (Washington, D.C.)* **1987**, *235*, 871.

0002-7863/87/1509-3656$01.50/0